On the Stefan Problem with Internal Heat Generation and Prescribed Heat Flux Conditions at the Boundary in Cylindrical Coordinates

A Thesis

Presented in Partial Fulfillment of the Requirements for the

Degree of Master of Science

with a

Major in Mathematics

in the

College of Graduate Studies

University of Idaho

by

Olufolahan Irene Ogidan

Major Professor: Lyudmyla Barannyk, Ph.D.

Committee Members: John Crepeau, Ph.D.; Gao Fuchang, Ph.D.

Department Administrator: Christopher Williams, Ph.D.

August 2019

Authorization to Submit Thesis

This thesis of Olufolahan Irene Ogidan, submitted for the degree of Master of Science with a major in Mathematics and titled "On the Stefan Problem with Internal Heat Generation and Prescribed Heat Flux Conditions at the Boundary in Cylindrical Coordinates", has been reviewed in final form. Permission, as indicated by the signatures and dates given below, is now granted to submit final copies to the College of Graduate Studies for approval.

Major Professor: _____Date_____
Lyudmyla Barannyk, Ph.D.

Committee Members: _____Date_____
John Crepeau, Ph.D.

_____Date_____
Fuchang Gao, Ph.D.

Department Administrator: _____Date_____
Christopher Williams, Ph.D.

Abstract

My thesis focuses on the evolution of the solid-liquid interface during melting and solidification in a material with constant internal heat generation and prescribed heat flux at the boundary in a cylinder. A phase change process in which a material transitions between two phases, solid and liquid, is known as a Stefan moving boundary problem.

We assume that the internal heat generation is constant and the same in both phases. The material properties in both phases are also taken to be constant and equal. We assume that the heat is transferred only by conduction and we neglect convection in the liquid phase. In addition, we assume that there is a sharp interface between two phases where the phase changes at a single melting temperature and there is no mushy zone at the interface. The presence of the internal heat generation makes the problem nonhomogeneous. Starting from the heat conduction equation, the approach finds steady-state and transient temperature solutions in each phase and employs the separation of variables technique to find transient solutions. A nonlinear first-order differential equation with Fourier-Bessel series terms is derived for the time-dependent motion of the interface. Analytic solutions for temperature profiles in each phase are derived. We do not introduce the Stefan number since there is only one fixed temperature: melting temperature. Instead we introduce dimensionless heat flux at the boundary. The initial value problem is solved numerically, and solutions compared to the previously derived quasi-steady ones. It is shown that when the internal heat generation and the heat flux at the boundary have a close range of values, it takes longer for the front to reach steady state than when the values are farther apart. As the difference between the internal heat generation and the flux increases, the transient solution becomes more dominant and the numerical solution of the phase change front does not reach steady-state before the outer boundary or centerline is reached. This shows that the prescribed heat flux can be used as a parameter that controls the motion of the interface. The problem has applications for a nuclear fuel rod during meltdown.

Acknowledgements

I would like to thank the Almighty God for the strength, wisdom and for the ability to understand, learn and complete this thesis.

I also will like to admire the help and guidance of my major professor Prof. Lyudmyla Barannyk. Your patience, motherly love and overall support were amazing. I pray for God to continually protect you and grant all your heart desires.

I am also grateful to my committee member Prof. John Crepeau who was always ready and available for every form of questions and guidance I needed. God bless you. I would also like to express my gratitude to my committee member Prof. Gao Fuchang who put in his time and efforts into this thesis. Your comments are suggestions were very helpful and made my thesis better.

Additionally, I would like to appreciate the mathematics department for granting me the opportunity and financial support to go through this thesis and my MS degree. Also, to the mathematics office staff: Jana Joyce, Melissa Gottschalk, Jaclyn Gotch and Jessica DeWitt. You all are the absolute best.

To my mum, Mrs I. M. Ogidan: thank you for all your words of encouragement, prayers and undying love. To my sister Bunmi: you are the best. To my cousin Gbenga Ige: thank you for your mentorship and support. God bless you. To my dad, Mr. A. Ogidan and my brothers Abiodun and Yinka, I love you all.

To my Moscow friends who became family, you all have been superb. Thank you.

Table of Contents

Nomenclature

Throughout the thesis, we use the following notations.

A_n, B_n Fourier Coefficients

c_p specific heat

Δh_f latent heat of fusion

k thermal conductivity

r_o distance from the center to the edge of the cylinder

$\dot{q}$ volumetric internal heat generation

J_0, Y_0 Bessel functions of 1st and 2nd kinds of order 0

J_1, Y_1 Bessel functions of 1st and 2nd kinds of order 1

$\dot{Q}$ dimensionless internal heat generation

Q'' nondimensional heat flux

s(t) distance to the phase change front

t time

T temperature

q''_o constant surface heat flux

T_m melt temperature

x,r distance

Greek Symbols

α thermal diffusivity

η nondimensional distance

ϕ initial temperature profile

Φ nondimensional initial temperature profile

λ_n, $\hat{\lambda_n}$ characteristic eigenvalues

θ nondimensional temperature

ρ density

τ nondimensional time

$\zeta(\tau)$ nondimensional distance to phase change front

z_{0n} zeros of Bessel function $J_0(z)$

[.] dimension of a quantity

Subscripts

liq liquid

sol solid

ss steady state

tr transient

List of Figures

CHAPTER 1

Introduction

1.1 History of Stefan Problem

Solid-liquid phase changes are encountered severally in nature and hence this solid-liquid phase change problem has been studied in various literature over the years. These studies were firstly carried out by Lamé and Clapeyron [1], then also by J. Stefan [2], whom these types of problems are associated with. Stefan solved the problem of the location and speed of the interface in a solid/liquid during melting or solidification. This kind of problems has now been extended over the years to include different cases like solidification of alloy systems, melting due to joule heating, laser irradiation [3] and so on. Rubenstein [4] proposes a different mathematical model for the solid/liquid phase change problems (Stefan problem). Burmeister [5] develops an accessible similarity solution to the phase change problem which shows the solid or liquid interface changes as the square root of time. Furzerland [6], Viswanath and Juluria [7] studied the difference between these two methods. Stefan problem is actively researched till date [8], [9].

In the Stefan problem two boundary conditions are imposed. The first one involves the temperature while the other is the energy balance. An important assumption in the formulation of Stefan problem is that there is a smooth surface which is the phase change boundary where one of the surfaces is the solid/liquid region and the other is the liquid/solid region [10]. The solid is recognized by its temperature which should be less than or equal to the equilibrium or melting temperature T_m, while the liquid area is recognized by its temperature which should be greater than or equal to T_m. The existence of this solid-liquid interface is a classic case which only occurs on special occasions such as solidification of pure metals or alloys with an appropriate amount of high temperature gradient.

In one directional solidification, it is known mathematically that in the presence of some conditions like absence of volumetric heat or unavailability of a mushy zone initially, that the

mushy region does not form until the solidification is complete. In two or more directional solidification, the presence of a sharp interface has been established to exist only for some period of time with suitable assumptions [11].

Regularly, a sharp interface separating a stable solid region from a stable liquid region decayed after a short time into a mushy region. The mushy region contains both solid and liquid phases and separates the stable solid region from the stable liquid region. The solid in the mushy region is present initially in the form of dendrites as shown in Fig. 1.1. The mushy area might also be formed during solidification if the liquid is supercooled or amid melting if the solid is superheated. This decay of sharp interface into a mushy area is ascribed to the morphological flimsiness of the solid-liquid interface.

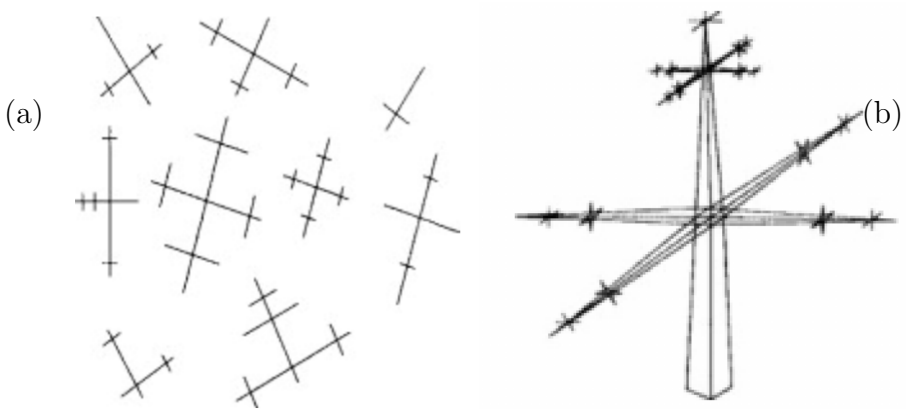

Figure 1.1: (a) Dendrites. (b) Formation of Dendrites [11]

1.2 Phase Change

Several mechanisms are at work when a liquid solidifies or a solid melts. This type of phenomena involves a change of phase which occurs with heat transfer. This heat transfer can be in any of these three modes: conduction, convection and radiation. *Conduction* is the transfer of heat energy by direct contact between objects, *convection* is the movement of heat by actual motion of matter which occurs in fluids while *radiation* is the transfer of energy with the help of electromagnetic waves. In many cases, materials go through these

phase changes by either taking in heat or emitting heat (latent heat). These changes occur due to changes in temperature either within or inside the material, determining the location and speed of solid/liquid interface during these changes (melting and solidification), which is the Stefan problem. In this types of problems, heat transfer is done by conduction and convection only, and the phase change temperature is carried out at a fixed temperature. Several applications of this kind of solid-liquid phase changes over a specified temperature ranges like water melting or freezing, molten lava solidifying, melting and solidification in metals casting procedures, like welding, brazing and soldering processes.

The effects of phase changes without internal heat generation are understood better than with internal heat generation. Viskanta [12] presents an overview and predictions for solidification and melting with reference to metals and metals processing. He shows that the phase front changes as the temperature changes and that there is a specific temperature region above which the whole material is entirely liquid or solid for alloy metals. He also did some research in the one directional phase change. His work gives a good introduction to the phase change problem. Viskanta also recognized the importance of convection, but saw it as trivial for metal processing problems especially the ones with slow changing phase front conditions. Yao and Prusa [13] gave reviews on conduction and convection dominant phase changes, enthalpy and other methods. They also discussed the complications in modeling of both melting/freezing processes and presented experimental results for melting in heated cylinders. In their work they assumed that none of the material generated internal heat.

Determining when and where the phase front is in either solidification or melting has been studied in various form over the years and different closed form solutions exist. Apart from this problem of phase front location, fluid movements can occur and cause convection currents which then increases heat transfer. A major problem is that in many materials there is not a specific location for the phase change front, but instead there is a "mushy zone" where the solid and liquid synchronize.

The classical Stefan problem involves heat transfer from external sources, phase changes

could also happen with internal heat generation. Some examples include geological heat transfer, nano-enhanced phase change and melting of nuclear fuel rod.

A nuclear meltdown occurs due to inadequate cooling of the nuclear fuel rods (see Fig. 1.2). This happens when the heat generated internally is greater than the heat removed by the nuclear cooling system to the extent that at least one of the fuel elements will develop temperature that exceeds its melting point. In these pressurized water reactors the melting of fuel rods can release radioactive elements and cause the zirconium cladding to react with water to generate explosive hydrogen [14].

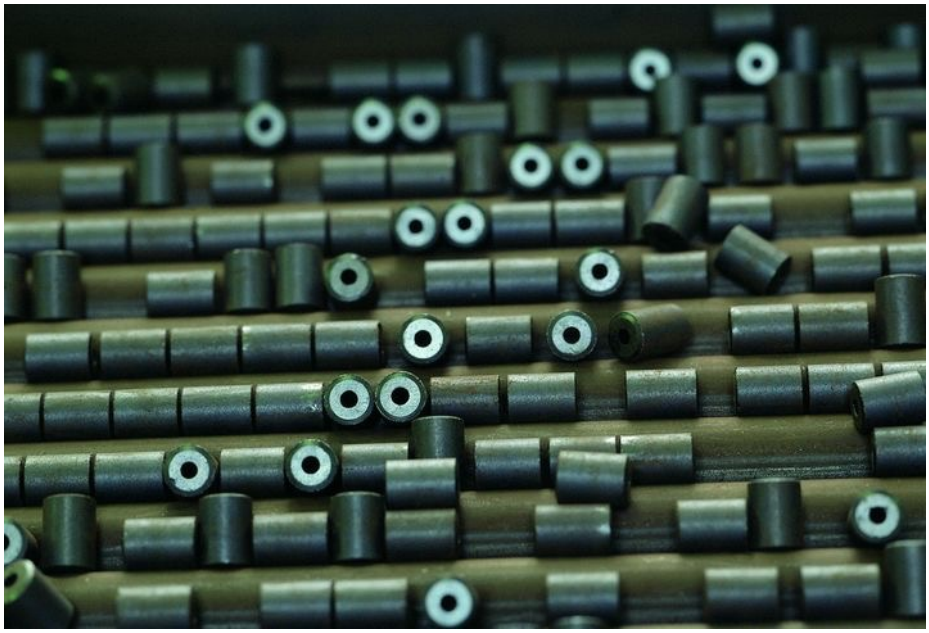

Figure 1.2: Nuclear fuel ceramic pellets [15]

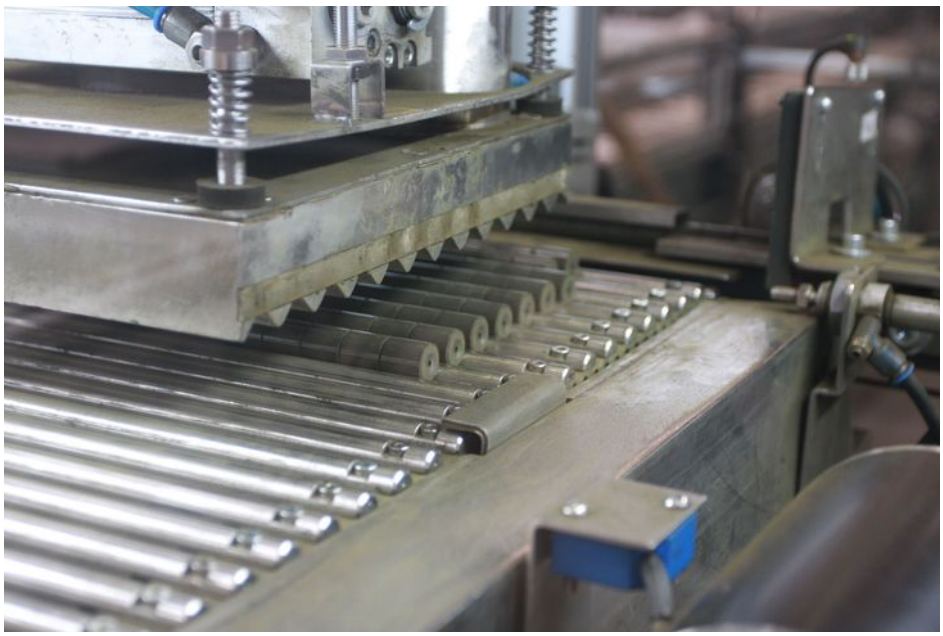

Figure 1.3: Nuclear fuel pellets installation into boxes [15]

A lot of exact solutions to the Stefan problem have been derived. Examples include problems with power-type latent heat [16], with prescribed heat flux at the boundary [17], with forced and natural convection [18]. Existence of solutions was investigated in [19]. In these and many other previous papers, the internal heat was not included.

Cheung et al. [20] worked on the processes of solidification and melting in heat-generating slabs bounded by two semi-infinite cold walls. Crepeau et al. [21] derived approximate solutions for the temperature and interface for materials with internal heat generation in plane wall, cylindrical, spherical and semi-infinite geometries by using a quasi-static approach. Furthermore, Crepeau et al. [22] investigated the solid-liquid phase change driven by volumetric energy generation in a vertical cylinder and showed excellent agreement between their quasi-static, approximate analytic and CFD (computational fluid dynamics) solutions for Stefan numbers less than one. Shrivastava et al. [23] used computational fluid dynamics to experiment with melting in materials with internal heat generation for a vertical cylinder. Numerical results showed good correlation with the experimental data. Barannyk et al. [24] studied the changes in the interface between the solid and liquid phases during melting and solidification of a material with constant internal heat generation and constant prescribed

temperature at the boundary in cylindrical coordinates. Analytical solutions which involved exponentially decaying Fourier-Bessel series were derived. The results were in an excellent correlation with quasi-static solutions for Stefan numbers less than one.

The research presented in this thesis addresses the Stefan problem in materials with internal heat generation and the prescribed heat flux at the boundary instead of constant temperature in cylindrical coordinates. The governing equation is derived for the interface between the two phases without making a quasi-static assumption and the resulting initial value problem is solved analytically and numerically. The results of the full problem are compared with quasi-static counterparts.

The rest of the thesis is organized as follows. In Chapter 2, we formulate the initial value boundary problem, change it to dimensionless variables, split solutions in each phase to transient and steady-state and solve it by the method of separation of variables and direct integration. This results in deriving a first order ordinary differential equation for the interface between liquid and solid phases, that involves Fourier-Bessel series. The eigenvalues in the liquid phase are related to the roots of the Bessel function $J_0(z)$ of the first kind of order zero. The associated eigenfunctions also involve $J_0(z)$. In the solid phase both eigenvalues and associated eigenfunctions are expressed in terms of both Bessel functions of first $J_0(z)$ and second $Y_0(z)$ kind. The eigenvalues are roots of a nonlinear equation. Temperature in both phases is also written in terms of infinite series. In Chapter 3, the interface equation is solved numerically as the initial value problem. The right hand side of this equation requires knowledge of temperature in both phases, in particular its derivative with respect of the spatial variable and evaluated at the interface. The eigenvalues in the solid phase are computed using asymptotic approximations of eigenvalues for large arguments using asymptotic results for Bessel functions for large arguments. Since Fourier-Bessel series are decaying in time and with the eigenvalue index, it is enough to use a few first terms in infinite series to approximate the solution. The obtained solutions are compared to quasi-static counterparts published earlier. We show that given the internal heat generation, the

value of the prescribed heat flux at the outer boundary of the cylinder can be used to control the motion of the interface. In Chapter 4, we provide conclusions.

CHAPTER 2

Derivation of Governing Equations

2.1 Problem Description

In this chapter, we set-up initial boundary value problem for temperature in both phases and derive a governing equation for the interface between phases.

The material is inside the cylinder of radius r_0. At time $t = 0$, we assume that there are two phases: liquid around the centerline and solid outside the liquid phase. Concentric symmetry is assumed. The schematic of the problem is shown in Fig. 2.1. In the solid and liquid phases, the changes in the temperature are driven by internal heat generation $\dot{q}$, while the heat flux q''_o at the outer boundary of the cylinder is kept constant. Temperature T_m is the melting temperature at the interface and the temperature gradient at the center line is zero by symmetry.

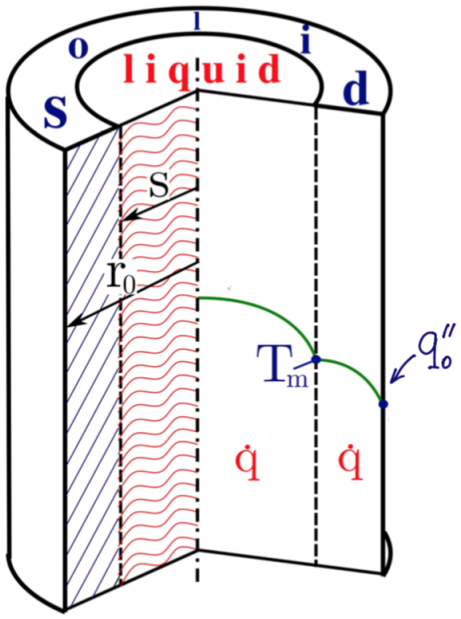

Figure 2.1: Schematic in cylindrical coordinates

We make the following assumptions:

1. The internal heat generation is constant and the same in both phases.

2. The temperature T_m of the phase change is fixed and known, since it is a property of the material.

3. The material properties in both phases are constant, uniform, and equal.

4. The heat transfer is by conduction and there is no convection in the liquid phase, all other effects are assumed negligible. The effect of convection is discussed in [25].

5. The phase change occurs at a single, constant temperature, T_m, so there is no "mushy zone" at the interface in between phases.

6. Density changes are also kept constant to avoid movement of the material.

2.2 Problem Formulation

Inside each phase, the evolution of temperature is governed by the heat equation [26]:

$$\begin{aligned} \frac{1}{r}\frac{\partial}{\partial r}\left(r\frac{\partial T(r,t)}{\partial r}\right) + \frac{\dot{q}}{k} &= \frac{1}{\alpha}\frac{\partial T}{\partial t} \\ 0 \leq s \leq r_0, \quad 0 \leq t \leq \infty & \end{aligned} \tag{2.1}$$

The liquid phase boundary and initial conditions are;

$$\begin{aligned} \frac{\partial T_{liq}(r,t)}{\partial r} &= 0 \\ T_{liq}(s(t),t) &= T_m \\ T_{liq}(r,0) &= \phi_{liq}(r) \end{aligned} \tag{2.2}$$

The first condition is the symmetry condition at $r = 0$, that follows from the assumption that the temperature profile in the liquid phase is parabolic with the centerline coinciding with its axis of symmetry. The second boundary condition is the continuity of temperature condition, where we assume that the material melts at temperature T_m. In the initial condition, $\phi_{liq}(r)$ is the initial temperature on the liquid phase.

Boundary and initial conditions in the solid phase are

$$\begin{aligned} T_{sol}(s(t),t) &= T_m \\ -k\frac{\partial T_{sol}(r,t)}{\partial r}\Big|_{r=r_0} &= q_0'' \\ T_{sol}(r,0) &= \phi_{sol}(r) \end{aligned} \tag{2.3}$$

Here the second condition specifies the heat flux at the outer boundary at $r = r_0$. In the initial condition, $\phi_{sol}(r)$ is the initial temperature in the solid phase.

While the interface equation is given by ([27], pg. 223) is derived due to the assumption that the the phase change occurs at a particular temperature and the two phases are seperated by a mixed-phase regions, this region consists of complex combined liquids and dendrites which is called the mushy region. An energy balance in the control volume which surrounds the fronts in both phases gives rise to the equation.

$$-k_{liq}\frac{\partial T_{liq}(r,t)}{\partial r}\Big|_{r=s(t)} + \rho_{sol}\Delta h_f\frac{ds(t)}{dt} = -k_{sol}\frac{\partial T_{sol}(r,t)}{\partial r}\Big|_{r=s(t)} \tag{2.4}$$

Where

$k_{liq}\dfrac{\partial T_{liq}(r,t)}{\partial r}\Big|_{r=s(t)}$: is the energy transferred into the control volume by conduction

$k_{sol}\dfrac{\partial T_{sol}(r,t)}{\partial r}\Big|_{r=s(t)}$: is the energy transferred out of the control volume by conduction

$\dfrac{ds(t)}{dt}$; is the interface velocity

2.3 Non-Dimensionalization and Derivation of Equations

It is convenient to study the problem under consideration in the dimensionless form. We rescale length variables by r_0, time scale is obtained from the heat equation (2.1) by balancing its first and last terms. Denote by [.] the dimension of a quantity (see, e.g. [28]). For example,

$[T]$ has dimension of temperature. Then the heat equation gives

$$\frac{1}{[r]}\frac{[k][r][T]}{[r]^2} = \rho c_p \frac{[T]}{[t]}$$

This gives us the time scale

$$t^* = \frac{{r_0}^2 \rho c_p}{k} = \frac{{r_0}^2}{\alpha}, \quad \text{where} \quad \alpha = \frac{k}{\rho c_p}$$

The temperature is rescaled using a typical temperature T^*. It is derived from the interface equation (2.4) by balancing the second and last terms in the following manner.

$$\rho_{sol}\Delta h_f \frac{[s]}{[t]} = k_{sol}\frac{[T]}{[r]}$$

Solving for $[T]$, we find

$$\frac{\rho_{sol}\Delta h_f}{k_{sol}}\frac{[s][r]}{[t]} = [T] = T^*$$

Using the time scale t^* and r_0 for length variables, we obtain the temperature scale

$$T^* = \frac{\rho_{sol}\Delta h_f \alpha}{t\, k_{sol}} = \frac{\Delta h_f}{c_p}$$

We introduce the following dimensionless variables

$$\begin{gathered} \eta = \frac{r}{r_0}, \quad \zeta(\tau) = \frac{s(t)}{r_0}, \quad \tau = \frac{\alpha t}{r_0^2} \\ \theta(\eta,\tau) = \frac{T(r,t) - T_m}{T^*}, \quad \dot{Q} = \frac{\dot{q}{r_o}^2}{\alpha \rho_{sol}\Delta_{hf}}, \quad Q'' = \frac{q'' r_0}{k_{sol} T^*} \end{gathered} \tag{2.5}$$

The last two are dimensionless internal heat generation and the heat flux at the boundary, whose derivation is shown below. Indeed,

In order to non-dimensionalize equations, we use the chain rule to find derivatives in

terms of new variables.

$$\frac{\partial}{\partial r} = \frac{\partial}{\partial \eta} \cdot \frac{d\eta}{dr} = \frac{1}{r_0}\frac{\partial}{\partial \eta}, \quad \frac{\partial}{\partial t} = \frac{\partial}{\partial \tau} \cdot \frac{d\tau}{dt} = \frac{\alpha}{{r_0}^2}\frac{\partial}{\partial \tau}$$

Heat equation becomes

$$\frac{1}{r_0 \eta}\frac{T^*}{{r_0}^2}\frac{\partial}{\partial \eta}\left(k r_0 \eta \frac{\partial \theta}{\partial \eta}\right) + \dot{q} = \rho c_p \frac{\alpha T^*}{{r_0}^2}\frac{\partial \theta}{\partial \tau}$$

We multiply the above equation by $\frac{{r_0}^2}{T^* K}$ and set $\dot{Q} = \frac{r_0^2 \dot{q}}{T^* k}$ to arrive at final form of the heat equation in dimensionless form:

$$\frac{1}{\eta}\frac{\partial}{\partial \eta}\left(\eta \frac{\partial \theta(\eta, \tau)}{\partial \eta}\right) + \dot{Q} = \frac{\partial \theta(\eta, \tau)}{\partial \tau} \tag{2.6}$$

Next we bring the boundary conditions to the dimensionless form.

$$\frac{\partial T_{liq}(r,t)}{\partial r}\Big|_{r=0} = 0 \quad \Rightarrow \quad \frac{T^*}{r_o}\frac{\partial \theta_{liq}(\eta,\tau)}{\partial \eta}\Big|_{\eta=0} = 0 \quad \Rightarrow \quad \frac{\partial \theta_{liq}(\eta,\tau)}{\partial \eta}\Big|_{\eta=0} = 0$$

$$T_{liq}(s(t), t) = T_m \quad \Rightarrow \quad \theta_{liq}(\eta, \tau)\Big|_{\eta=\zeta(\tau)} = 0$$

Then we consider the initial condition.

$$T_{liq}(r, 0) = \phi_{liq}(r) \quad \Rightarrow \quad \frac{T_{liq}(r,0) - T_m}{T^*} = \frac{\phi_{liq}(r) - T_m}{T^*} \stackrel{\text{def}}{=} \Phi_{liq}(\eta)$$

where $\Phi_{liq}(\eta)$ is the initial condition in the liquid phase in dimensionless variables.

Boundary and initial conditions in the solid phase are treated similarly.

$$T_{sol}(s(t), t) = T_m \quad \Rightarrow \quad \theta_{sol}(\zeta(\tau), \tau) = 0$$

$$\frac{\partial T_{sol}(r,t)}{\partial r}\Big|_{r=r_0} = -\frac{q_0''}{k_{sol}} \quad \Rightarrow \quad \frac{T^*}{r_o}\frac{\partial \theta_{sol}(\eta,\tau)}{\partial \eta}\Big|_{\eta=1} = -\frac{q_0''}{k_{sol}}$$

Let

$$Q'' = \frac{q'' r_0}{k_{sol} T^*}$$

Then

$$\frac{\partial \theta_{sol}(\eta, \tau)}{\partial \eta}\Big|_{\eta=1} = -\frac{q_0'' r_0}{k_{sol} T^*} \quad \Rightarrow \quad \frac{\partial \theta_{sol}(\eta, \tau)}{\partial \eta}\Big|_{\eta=1} = -Q''$$

The initial condition

$$T_{sol}(r, 0) = \phi_{sol}(r)$$

gives

$$\frac{T_{sol}(r, 0) - T_m}{T^*} = \frac{\phi_{sol}(r) - T_m}{T^*} \stackrel{\text{def}}{=} \Phi_{sol}(\eta)$$

The dimensionless interface equation is

$$\frac{k_{liq} T^*}{r_0} \frac{d\theta}{d\eta} + \frac{\alpha \rho_{sol} \Delta h_f}{r_0^2} \frac{d\zeta(\tau)}{d\tau} = \frac{k_{sol} T^*}{r_0} \frac{d\theta}{d\eta}$$

Multiply both sides of this equation by $\frac{r_0}{kT^*}$. This would make the coefficient of $\frac{d\zeta(\tau)}{d\tau}$ to be 1, so we do not need to introduce the Stefan number. This makes sense since we only have one temperature fixed: the melting temperature T_m. In order to introduce the Stefan number, we would need another fixed temperature so that we can consider their difference. We do not have it since instead we have a fixed derivative of the temperature at the outer boundary in terms of the heat flux.

To summarize, we write down problems in the liquid and solid phases in dimensionless form.

2.4 Problem in Dimensionless Form

Dimensionless liquid phase problem:

$$\begin{aligned} \frac{1}{\eta}\frac{\partial}{\partial\eta}\left(\eta\frac{\partial\theta_{liq}(\eta,\tau)}{\partial\eta}\right)+\dot{Q} &= \frac{\partial\theta_{liq}(\eta,\tau)}{\partial\tau} \\ \frac{\partial\theta_{liq}(\eta,\tau)}{\partial\eta}\Big|_{\eta=0} &= 0 \\ \theta_{liq}(\eta,\tau)\Big|_{\eta=\zeta(\tau)} &= 0 \\ \Phi_{liq}(\eta,0) &= \frac{\phi_{liq}(r)-T_m}{T^*} \end{aligned} \tag{2.7}$$

Dimensionless solid phase problem is

$$\begin{aligned} \frac{1}{\eta}\frac{\partial}{\partial\eta}\left(\eta\frac{\partial\theta_{sol}(\eta,\tau)}{\partial\eta}\right)+\dot{Q} &= \frac{\partial\theta_{sol}(\eta,\tau)}{\partial\tau} \\ \theta_{sol}(\eta,\tau)\Big|_{\eta=\zeta(\tau)} &= 0 \\ \frac{\partial\theta_{sol}(\eta,\tau)}{\partial\eta}\Big|_{\eta=1} &= 0 \\ \Phi_{sol}(\eta,0) &= \frac{\phi_{sol}(r)-T_m}{T^*} \end{aligned} \tag{2.8}$$

Dimensionless interface equation is

$$\frac{d\theta_{liq}(\eta,\tau)}{d\eta}\Big|_{\eta=\zeta(\tau)}+\frac{d\zeta(\tau)}{d\tau}=\frac{d\theta_{sol}(\eta,\tau)}{d\eta}\Big|_{\eta=\zeta(\tau)} \tag{2.9}$$

Equation (2.9) is a first order nonhomogeneous ordinary differential equation for the interface $\zeta(\tau)$. In order to determine the evolution of the interface, we need to know temperature in both solid and liquid phases. We find temperature separately in each phase. Solutions are computed by splitting them into transient and steady parts. The transient problem is homogeneous and we solve it using the method of separation of variables [29, 26]. The steady state problem is nonhomogeneous and we solve it by direct integration.

2.5 Solution in the Liquid Phase

The problem (2.7) is a nonhomogeneous initial boundary value problem. In order to solve it, we split it into a homogeneous problem with a transient solution $\theta_{liq,tr}(\eta,\tau)$ that satisfies the homogeneous equation and homogeneous boundary conditions, and a nonhomogeneous steady state problem with a solution $\theta_{liq,ss}(\eta)$. Therefore, we can write a solution to the full problem in the liquid phase as a sum of the transient solution $\theta_{liq,tr}(\eta,\tau)$ and steady state solution $\theta_{liq,ss}(\eta,\tau)$:

$$\theta_{liq}(\eta,\tau) = \theta_{liq,tr}(\eta,\tau) + \theta_{liq,ss}(\eta)$$

Transient solution $\theta_{liq}(\eta,\tau)$ satisfies the homogeneous heat equation

$$\frac{1}{\eta}\frac{\partial}{\partial\eta}\left(\eta\frac{\partial\theta_{liq,tr}(\eta,\tau)}{\partial\eta}\right) = \frac{\partial\theta_{liq,tr}(\eta,\tau)}{\partial\tau} \tag{2.10}$$

with homogeneous boundary and corresponding initial conditions:

$$\theta_{liq,tr}(\zeta(\tau),\tau) = 0, \quad \frac{\partial\theta_{liq,tr}(\eta,\tau)}{\partial\eta}\Big|_{\eta=0} = 0$$

$$\theta_{liq}(\eta,0) = \phi_{liq}(\eta) - \theta_{liq,ss}(\eta)$$

To find the transient solution, we use the method of separation of variables [29, 26]. We assume that the solution can be written as a product of two functions: function of η alone and a function of τ alone, i.e. we let

$$\theta_{liq,tr}(\eta,\tau) = f(\eta)g(\tau)$$

Substituting this into the heat equation (2.10)

$$\frac{1}{\eta}\frac{d}{d\eta}\left(\eta\frac{df}{d\eta}\right)g(\tau) = f(\eta)\frac{dg}{d\tau} \quad \Big| \quad \frac{1}{fg}$$

and separating variables, we find

$$\frac{1}{\eta f}\frac{d}{d\eta}\left(\eta\frac{df}{d\eta}\right) = \frac{\frac{dg}{d\tau}}{g} = -\lambda^2$$

where $-\lambda^2$ is a separation constant. We can show that this constant has to be negative to get a physically consistent solution.

The τ-dependent problem

$$\frac{dg}{d\tau} = -\lambda^2 g$$

has a solution

$$g(\tau) = c\,\mathrm{e}^{-\lambda^2\tau}$$

where c is an arbitrary constant of integration.

Next consider the spatial η-dependent problem

$$\frac{1}{\eta f}\frac{d}{d\eta}\left(\eta\frac{df}{d\eta}\right) + \lambda^2 = 0 \quad \Big| \quad \eta^2 f$$

$$\eta\frac{d}{d\eta}\left(\eta\frac{df}{d\eta}\right) + \lambda^2\eta^2 f = 0$$

$$\eta\left(\frac{df}{d\eta} + \eta\frac{d^2 f}{d\eta^2}\right) + \lambda^2\eta^2 f = 0$$

Introduce change of variables $z = \lambda\eta$. Then

$$\frac{d}{d\eta} = \frac{d}{dz}\frac{dz}{d\eta} = \lambda\frac{d}{dz}$$

and we arrive at

$$z^2\frac{d^2 f}{d\eta^2} + z\frac{df}{dz} + z^2 f = 0 \tag{2.11}$$

which is the Bessel equation of order 0. Its general solution is

$$F(\eta) = c_1 J_0(\lambda\eta) + c_2 Y_0(\lambda\eta) \tag{2.12}$$

where $J_0(z)$ and $Y_0(z)$ are Bessel functions of first and second kind, respectively, of order 0; c_1, c_2 are arbitrary constants. The graphs of the Bessel functions $J_0(z)$ and $Y_0(z)$ are shown in Fig. 2.2. We can see that function $J_0(z)$ is bounded at $z = 0$ whereas Y_0 is not bounded and it goes to minus infinity as z approaches 0. The derivative of Y_0 is also unbounded at $z = 0$.

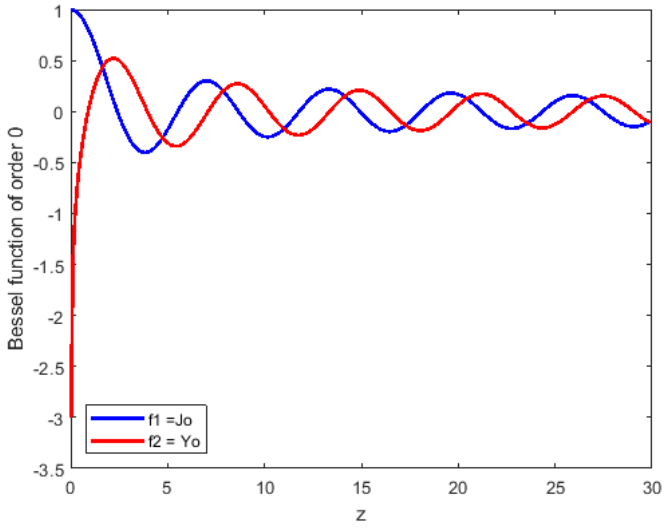

Figure 2.2: Bessel functions $J_0(z)$ and $Y_0(z)$ of order 0

Boundary condition $\left.\frac{df}{dz}\right|_{z=0} = 0$ implies that $c_2 = 0$. We can also argue here that the temperature at $z = 0$ has to be bounded, which would eliminate function $Y_0(z)$ as well. The condition $\theta_{liq,tr}(\zeta(\tau), \tau) = 0$ implies $f(\lambda\zeta) = 0$, hence $c_1 J_0(\lambda\eta) = 0$. For a nontrivial solution, $c_1 \neq 0$, hence, $J_0(\lambda\eta) = 0$ or $\lambda\zeta = z_{0n}$, $n = 1, 2, \ldots$. Here z_{0n} is the n^{th} zero of $J_0(z)$. This gives us eigenvalues

$$\lambda_n = \frac{z_{0n}}{\zeta(\tau)}, \quad n = 1, 2, \ldots$$

with associated eigenfunctions

$$F_n(\eta) = J_0(\lambda_n \eta) = J_0\left(\frac{z_{0n}}{\zeta(\tau)}\eta\right), \quad n = 1, 2, \ldots$$

Using the principle of linear superposition, we can write the transient solution in the form

of an infinite series

$$\theta_{liq,tr}(\eta,\tau) = \sum_{n=1}^{\infty} A_n J_0(\lambda_n \eta)\, \mathrm{e}^{-\lambda_n^2 \tau}$$

where A_n are coefficients that we find using the initial condition and orthogonality of eigenfunctions $J_0(\lambda_n \eta)$.

At time $\tau = 0$,

$$\theta_{liq,tr}(\eta,0) = \Phi_{liq}(\eta) - \theta_{liq,ss}(\eta) = \sum_{n=1}^{\infty} A_n J_0(\lambda_n \eta) \tag{2.13}$$

Equation (2.13) shows that $\theta_{liq,tr}(\eta,0)$ is a Fourier-Bessel series with coefficients A_n. Multiply both sides by $J_0(\lambda_n \eta)\,\eta$ and integrate over $0 \le \eta \le \zeta$. Bessel functions $J_0(\lambda_n \eta)$ are orthogonal on $[0, \zeta(\tau)]$ with weight function η, that is

$$\int_0^{\zeta(\tau)} J_0(\lambda_n \eta) J_0(\lambda_m \eta) \eta \, d\eta = 0, \quad n \neq m$$

therefore, we can find Fourier-Bessel coefficients

$$A_n = \frac{\int_0^{\zeta(\tau)} [\Phi_{liq}(\eta) - \theta_{liq,ss}(\eta)] J_0(\lambda_n \eta) \eta \, d\eta}{\int_0^{\zeta(\tau)} J_0^2(\lambda_n \eta) \eta \, d\eta}$$

Fourier type series solutions of this kind of problems have been derived in the case of cartesian coordinates [30, 24]. Power series solutions were used to solve one dimensional Stefan problem with variable latent heat and single phase Stefan problem [31, 32]. In our case, because of the cylindrical geometry of our problem, it is convenient to express the solution in terms of Fourier-Bessel series and use orthogonality of Bessel functions to efficiently compute Fourier-Bessel coefficients.

The liquid steady-state problem consists of

$$\frac{1}{\eta} \frac{d}{d\eta} \left(\eta \frac{d\theta_{liq,ss}(\eta)}{d\eta} \right) + \dot{Q} = 0 \tag{2.14}$$

with the boundary conditions given as

$$\theta_{liq,ss}(s(\tau)) = 0, \quad \frac{d\theta_{liq,ss}(\eta)}{d\eta}\Big|_{\eta=0} = 0$$

Multiplying both sides of equation (2.14) by η, we get

$$\frac{d}{d\eta}\left(\eta\frac{d\theta_{liq,ss}(\eta)}{d\eta}\right) = -\eta\dot{Q}$$

Integrate it once

$$\eta\frac{d\theta_{liq,ss}(\eta)}{d\eta} = -\frac{\eta^2}{2}\dot{Q} + c_1$$

where c_1 is an arbitrary constant of integration. Since $\frac{d\theta}{d\eta} = 0$ at $\eta = 0$, we get $c_1 = 0$. Divide both sides of the resulting equation by η:

$$\eta\frac{d\theta_{liq,ss}(\eta)}{d\eta} = -\frac{\eta^2}{2}Q \quad \Big|\frac{1}{\eta}$$

Then

$$\frac{d\theta_{liq,ss}(\eta)}{d\eta} = -\frac{\eta}{2}\dot{Q}$$

Integrate again to obtain

$$\theta_{liq,ss}(\eta) = -\frac{\eta^2}{4}\dot{Q} + c_2$$

where c_2 is another constant of integration. At the interface $\eta = \zeta$,

$$\theta_{liq,ss}(\zeta) = -\frac{\zeta^2}{4}\dot{Q} + c_2 = 0 \Rightarrow c_2 = \frac{\zeta^2}{4}\dot{Q}$$

Therefore,

$$\theta_{liq,ss}(\eta) = \frac{\eta^2}{4} + \frac{\zeta^2}{4}\dot{Q} = \frac{\zeta^2 - \eta^2}{4}\dot{Q} = \frac{\dot{Q}}{4}(\zeta^2(\tau) - \eta^2)$$

Adding transient and steady state solutions, we obtain temperature in the liquid phase:

$$\theta_{liq}(\eta,\tau) = \sum_{n=1}^{\infty} A_n \, \mathrm{e}^{-\lambda_n^2 \tau} \, f_n(\lambda_n \eta) + \theta_{liq,ss}(\eta) \tag{2.15}$$

where

$$\theta_{liq,ss}(\eta) = \frac{\dot{Q}}{4}(\zeta^2(\tau) - \eta^2)$$

$$A_n = \frac{\int_0^{\zeta(\tau)} [\Phi_{liq}(\eta) - \theta_{liq,ss}(\eta)] J_0(\lambda_n \tau) \eta \, d\eta}{\int_0^{\zeta(\tau)} J_0^2(\lambda_n \eta) \eta \, d\eta}$$

$$\lambda_n = \frac{z_{0n}}{\zeta(\tau)}, \quad f_n(\eta) = J_0(\lambda_n \eta), \quad n = 1, 2, \ldots$$

2.6 Solution in the Solid Phase

We use the same approach here as for the liquid phase. We separate solution into transient and steady state parts by writing

$$\theta_{sol}(\eta,\tau) = \theta_{sol,tr}(\eta,\tau) + \theta_{sol,ss}(\eta)$$

The transient solution $\theta_{sol,tr}(\eta,\tau)$ satisfies

$$\frac{1}{\eta}\frac{\partial}{\partial \eta}\left(\eta \frac{\partial \theta_{sol,tr}(\eta,\tau)}{\partial \eta}\right) = \frac{\partial \theta_{sol,tr}(\eta,\tau)}{\partial \tau}$$

with the boundary and initial conditions given as

$$\theta_{sol,tr}(\zeta(\tau),\tau) = 0, \quad \frac{\partial \theta_{sol,tr}(\eta,\tau)}{\partial \eta}\Big|_{\eta=1} = 0$$

$$\theta_{sol,tr}(\eta,0) = \phi_{sol}(\eta) - \theta_{sol,ss}(\eta)$$

We use the method of separation of variables to solve transient problem and assume the solution $\theta_{sol,tr}(\eta,\tau)$ as a product of two functions:

$$\theta_{sol,tr}(\eta,\tau) = f(\eta)g(\tau)$$

Separating variables with a separation constant $-\lambda^2$, we obtain the τ-dependent problem

$$\frac{dg}{d\tau} = -\lambda^2 g$$

whose solution is

$$g(\tau) = c\,\mathrm{e}^{-\lambda^2\tau}$$

Here c is an arbitrary constant.

The η-dependent problem consists of the same equation as in the liquid phase

$$\eta\frac{df}{d\eta} + \eta^2\frac{d^2f}{d\eta^2} + \lambda^2\eta^2 f = 0, \quad \zeta \le \eta \le 1$$

that with the help of substitution $z = \lambda\eta$ transforms into the same Bessel equation of order 0:

$$z^2\frac{d^2f}{d\eta^2} + z\frac{df}{dz} + z^2 f = 0$$

with the general solution

$$f(z) = c_1 J_0(z) + c_2 Y_0(z)$$

where $J_0(z)$ and $Y_0(z)$ are Bessel functions of first and second kind, respectively. Since the domain now is away from the origin, both functions $J_0(z)$ and $Y_0(z)$ are part of the solution. Going back to variable η, we can write

$$f(\lambda\eta) = c_1 J_0(\lambda\eta) + c_2 Y_0(\lambda\eta) \tag{2.16}$$

The boundary condition $f(\eta)\Big|_{\eta=\zeta} = 0$ implies

$$c_1 J_0(\zeta(\tau)\lambda) + c_2 Y_0(\zeta(\tau)\lambda) = 0 \tag{2.17}$$

To use the other boundary condition

$$\frac{df}{d\eta}\Big|_{\eta=1} = 0$$

we need to differentiate Bessel functions. It is known [26] that

$$J_0'(z) = -J_1(z), \quad Y_0'(z) = -Y_1(z)$$

Then

$$\frac{df}{d\eta} = -c_1\lambda J_1(\lambda\eta) - c_2\lambda Y_1(\lambda\eta)$$

evaluating this equation at $\eta = 1$, we get

$$\frac{df}{d\eta}\Big|_{\eta=1} = -\lambda(c_1 J_1(\lambda) - c_2 Y_1(\lambda)) = 0 \quad \Big|\frac{1}{\lambda}$$

Dividing this equation by λ and using the result from the first boundary condition (2.17), we arrive at the system

$$c_1 J_1(\lambda) + c_2 Y_1(\lambda) = 0$$

$$c_1 J_0(\zeta(\tau)\lambda) + c_2 Y_0(\zeta(\tau)\lambda) = 0$$

for c_1 and c_2. To find a condition for a nontrivial solution to exist, we write this system in a matrix form

$$\begin{bmatrix} J_0(\zeta\lambda) & Y_0(\zeta\lambda) \\ J_0(\lambda) & Y_1(\lambda) \end{bmatrix} \begin{bmatrix} c_1 \\ c_2 \end{bmatrix} = \begin{bmatrix} 0 \\ 0 \end{bmatrix} \tag{2.18}$$

For a homogeneous linear system to have a nontrivial solution, the determinant of the coef-

ficient matrix has to be 0, i.e.

$$Y_1(\lambda)J_0(\zeta\lambda) - Y_0(\zeta\lambda)J_1(\lambda) = 0 \tag{2.19}$$

This is a nonlinear equation. Its roots are eigenvalues $\tilde{\lambda}_n$ that form an infinite sequence as n increases. Once we know eigenvalues $\tilde{\lambda}_n$, we can find corresponding eigenfunctions. Since

$$c_1 J_1(\lambda) + c_2 Y_1(\lambda) = 0$$

we solve for c_2 in terms of c_1:

$$c_1 J_1(\lambda) = -c_2 Y_1(\lambda) \quad \Rightarrow \quad c_2 = -c_1 \frac{J_1(\lambda)}{Y_1(\lambda)}$$

Substituting this into (2.16), we find

$$f(\lambda\eta) = c_1 \left[J_0(\lambda\eta) - \frac{J_1(\lambda)}{Y_1(\lambda)} Y_0(\lambda\eta) \right]$$

Hence,

$$\tilde{f}_n(\tilde{\lambda}_n\eta) = J_0(\tilde{\lambda}_n\eta) - \frac{J_1(\tilde{\lambda}_n)}{Y_1(\tilde{\lambda}_n)} Y_0(\tilde{\lambda}_n\eta)$$

are the eigenfunctions with the corresponding eigenvalues $\tilde{\lambda}_n$.

Using the principle of linear superposition, we write the transient solution as an infinite series

$$\theta_{sol,tr}(\eta,\tau) = \sum_{n=1}^{\infty} B_n \, \mathrm{e}^{-\tilde{\lambda}_n^2 \tau} \, \tilde{f}_n(\tilde{\lambda}_n\eta) \tag{2.20}$$

where coefficients B_n are computed using the initial condition at $\tau = 0$:

$$\theta_{sol,tr}(\eta,0) = \Phi_{sol}(\eta) - \theta_{sol,ss}(\eta) = \sum_{n=1}^{\infty} B_n \tilde{f}_n(\tilde{\lambda}_n\eta)$$

Using orthogonality of eigenfunctions $\tilde{f}_n(\tilde{\lambda}_n\eta)$ on the interval $[\zeta, 1]$ with the weight function

η, we find

$$B_n = \frac{\int_{\zeta(\tau)}^{1} [\Phi_{sol}(\eta) - \theta_{sol,ss}(\eta)] \tilde{f}_n(\tilde{\lambda}_n \eta) \eta \, d\eta}{\int_{\zeta(\tau)}^{1} \tilde{f}_n{}^2(\tilde{\lambda}_n \eta)) \eta \, d\eta}, \quad n = 1, 2, \ldots$$

The steady state part $\theta_{sol,ss}(\eta)$ satisfies the equation

$$\frac{1}{\eta} \frac{d}{d\eta} \left(\eta \frac{d\theta_{sol,ss}(\eta)}{d\eta} \right) + \dot{Q} = 0 \tag{2.21}$$

with the boundary conditions

$$\theta_{sol,ss}(\zeta(\tau)) = 0, \quad \frac{\partial \theta_{sol,ss}(\eta)}{\partial \eta}\Big|_{\eta=1} = -Q''$$

Multiplying both sides of equation (2.21) by η

$$\frac{d}{d\eta} \left(\eta \frac{d\theta_{sol,ss}(\eta)}{d\eta} \right) = -\eta \dot{Q}$$

and integrating the result once, we get

$$\eta \frac{d\theta_{sol,ss}(\eta)}{d\eta} = -\frac{\eta^2}{2} \dot{Q} + c_1$$

Since $\frac{d\theta}{d\eta} = -Q''$ at $\eta = 1$, we find

$$c_1 = \frac{\dot{Q}}{2} - Q''$$

Hence,

$$\frac{d\theta_{sol,ss}(\eta, \tau)}{d\eta} = -\frac{\eta}{2} \dot{Q} + \frac{c_1}{\eta}$$

Integrate again

$$\theta_{sol,ss}(\eta) = -\frac{\eta^2}{4} \dot{Q} + c_1 \ln \eta + c_2$$

Since

$$0 = \theta(\eta)|_{\eta=\zeta} = \frac{\zeta^2}{4} \dot{Q} + c_1 \ln \zeta + c_2$$

we have

$$c_2 = \frac{\zeta^2}{4}\dot{Q} - c_1 \ln \zeta = \frac{\zeta^2}{4}\dot{Q} - \left(\frac{\dot{Q}}{2} - Q''\right) \ln \zeta$$

Finally,

$$\theta_{sol,ss}(\eta) = -\frac{\eta^2}{4}\dot{Q} + \left(\frac{\dot{Q}}{2} - Q''\right) \ln \eta + \frac{\zeta^2}{4}\dot{Q} - \left(\frac{\dot{Q}}{2} - Q''\right) \ln \zeta$$

or

$$\theta_{sol,ss}(\eta) = \frac{\dot{Q}}{4}\left(\zeta^2(\tau) - \eta^2\right) + \left(\frac{\dot{Q}}{2} - Q''\right) \ln \frac{\eta}{\zeta} \tag{2.22}$$

Therefore, temperature in the solid phase is:

$$\theta_{sol}(\eta, \tau) = \sum_{n=1}^{\infty} B_n \tilde{f}_n(\tilde{\lambda}_n \eta)\, \mathrm{e}^{-\tilde{\lambda}^2 \tau} + \theta_{sol,ss}(\eta) \tag{2.23}$$

where

$$B_n = \frac{\int_{\zeta(\tau)}^{1} (\Phi_{sol}(\eta) - \theta_{sol,ss}(\eta)) \tilde{f}_n(\tilde{\lambda}_n \eta) \eta \, d\eta}{\int_{\zeta(\tau)}^{1} [\tilde{f}_n(\tilde{\lambda}_n \eta)]^2 \eta \, d\eta}$$

$$\tilde{f}_n(\tilde{\lambda}_n \eta) = J_0(\tilde{\lambda}_n \eta) - \frac{J_1(\tilde{\lambda}_n)}{Y_1(\tilde{\lambda}_n)} Y_0(\tilde{\lambda}_n \eta)$$

$\theta_{sol,ss}(\eta)$ is given in (2.22).

Since eigenvalues $\tilde{\lambda}_n$, $n = 1, 2, \ldots$ are roots of the nonlinear equation (2.19), it is useful to recall asymptotic properties of Bessel functions. We will use them to find approximate locations of the roots. This information is employed in Chapter 3 to compute eigenvalues numerically.

2.7 Asymptotic Properties of Bessel Functions

Bessel functions have been studied extensively [26, 33, 34]. Asymptotic formulae for small and large arguments are helpful in understanding the behavior of the special functions in these two regimes. The asymptotic results for small arguments demonstrate that Bessel functions of the first kind are bounded whereas the functions of the second kind are unbounded

as the argument approaches zero.

Asymptotic formulae of Bessel functions of the first and second kinds, respectively, for small z are

$$J_n(z) \simeq \begin{cases} 1, & n = 0 \\ \frac{1}{2^n n!} z^n, & n > 0 \end{cases}$$

$$Y_n(z) \simeq \begin{cases} \frac{2}{\pi} \ln z, & n = 0 \\ -\frac{2^n (n-1)!}{\pi} z^{-n}, & n > 0 \end{cases}$$

In particular, these results show that $J_0 \simeq 1$ and $Y_0 \simeq \ln z$ as $z \to 0$, which explains our choice of constants c_1 and c_2 in finding transient solutions.

Asymptotic properties for large z are given by formulae

$$J_n(z) \simeq \sqrt{\frac{2}{\pi z}} \cos\left(z - \frac{\pi n}{2} - \frac{\pi}{4}\right), \quad z \to \infty \tag{2.24}$$

$$Y_n(z) \simeq \sqrt{\frac{2}{\pi z}} \sin\left(z - \frac{\pi n}{2} - \frac{\pi}{4}\right), \quad z \to \infty \tag{2.25}$$

We can see that Bessel functions behave like periodic cosine and sine functions but with the amplitude decaying inversely proportionally to $\sqrt{z}$. These results can be used to study approximate location of the roots of Bessel functions. They can be employed either as initial guesses in root finding methods or to determine an interval on which each root is. Indeed, when eigenvalues $\tilde{\lambda}_n$ are large, the arguments of Bessel functions in equation (2.19) or in equation

$$Y_1(\tilde{\lambda}_n) J_0(\zeta \tilde{\lambda}_n) - Y_0(\zeta \tilde{\lambda}_n) J_1(\tilde{\lambda}_n) = 0 \tag{2.26}$$

are large. Using results (2.24) and (2.25), we can write

$$J_0(z) \simeq \sqrt{\frac{2}{\pi z}} \cos\left(z - \frac{\pi}{4}\right), \quad Y_0(z) \simeq \sqrt{\frac{2}{\pi z}} \sin\left(z - \frac{\pi}{4}\right)$$

$$J_1(z) \simeq \sqrt{\frac{2}{\pi z}} \cos\left(z - \frac{\pi}{2} - \frac{\pi}{4}\right) = \sqrt{\frac{2}{\pi z}} \sin\left(z - \frac{\pi}{4}\right)$$

$$Y_1(z) \simeq \sqrt{\frac{2}{\pi z}} \sin\left(z - \frac{\pi}{2} - \frac{\pi}{4}\right) = -\sqrt{\frac{2}{\pi z}} \cos\left(z - \frac{\pi}{4}\right)$$

So, at $z = \tilde{\lambda}\zeta$ or $z = \tilde{\lambda}$ we have

$$J_0(\tilde{\lambda}\zeta) \simeq \sqrt{\frac{2}{\pi\tilde{\lambda}\zeta}} \cos\left(\tilde{\lambda}\zeta - \frac{\pi}{4}\right), \quad Y_0(\tilde{\lambda}\zeta) \simeq \sqrt{\frac{2}{\pi\tilde{\lambda}\zeta}} \sin\left(\tilde{\lambda}\zeta - \frac{\pi}{4}\right)$$

$$J_1(\tilde{\lambda}) \simeq \sqrt{\frac{2}{\pi\tilde{\lambda}}} \sin\left(\tilde{\lambda} - \frac{\pi}{4}\right), \quad Y_1(\tilde{\lambda}) \simeq -\sqrt{\frac{2}{\pi\tilde{\lambda}}} \cos\left(\tilde{\lambda} - \frac{\pi}{4}\right)$$

Substituting these asymptotic results in equation (2.26), we obtain

$$-\sqrt{\frac{2}{\pi\tilde{\lambda}\zeta}} \cos\left(\tilde{\lambda}\zeta - \frac{\pi}{4}\right) \sqrt{\frac{2}{\pi\tilde{\lambda}}} \cos\left(\tilde{\lambda} - \frac{\pi}{4}\right) - \sqrt{\frac{2}{\pi\tilde{\lambda}}} \sin\left(\tilde{\lambda} - \frac{\pi}{4}\right) \sqrt{\frac{2}{\pi\tilde{\lambda}\zeta}} \sin\left(\tilde{\lambda}\zeta - \frac{\pi}{4}\right) = 0$$

or

$$-\frac{2}{\pi\tilde{\lambda}\sqrt{\zeta}} \left[\cos\left((\tilde{\lambda}\zeta - \frac{\pi}{4}\right) \cos\left(\tilde{\lambda} - \frac{\pi}{4}\right) + \sin\left(\tilde{\lambda} - \frac{\pi}{4}\right) \sin\left(\tilde{\lambda}\zeta - \frac{\pi}{4}\right)\right] = 0$$

But $-\frac{2}{\pi\tilde{\lambda}\sqrt{\zeta}} \neq 0$, then using trigonometric formula $\cos(a-b) = \cos a \cos b + \sin a \sin b$ with $a = \tilde{\lambda}\zeta - \frac{\pi}{4}$ and $b = \tilde{\lambda} - \frac{\pi}{4}$, we can write

$$\cos\left(\tilde{\lambda}\zeta - \frac{\pi}{4} - \left(\tilde{\lambda} - \frac{\pi}{4}\right)\right) = 0$$

or

$$\cos(\tilde{\lambda}(1-\zeta)) = 0$$

whose roots are

$$\tilde{\lambda}_n^{as}(1-\zeta) = \frac{\pi}{2} + \pi(n-1), \quad n = 1, 2, \ldots$$

or

$$\tilde{\lambda}_n^{as} = \frac{-\frac{\pi}{2} + \pi n}{1-\zeta}, \quad n = 1, 2, \ldots \tag{2.27}$$

Here $\tilde{\lambda}_n^{as}$ are roots of an asymptotic approximation the left hand side of (2.26) for large arguments. Result (2.27) shows that the eigenvalues $\tilde{\lambda}_n$ in the solid phase are approximately

$$\tilde{\lambda}_n \approx \tilde{\lambda}_n^{as} = \frac{-\frac{\pi}{2} + \pi n}{1-\zeta}, \quad n = 1, 2, \ldots \tag{2.28}$$

In particular, the distance between successive roots is

$$\tilde{\lambda}_{n+1} - \tilde{\lambda}_n \approx \frac{-\frac{\pi}{2} + \pi(n+1)}{1-\zeta} - \frac{-\frac{\pi}{2} + \pi n}{1-\zeta} = \frac{\pi}{1-\zeta} \tag{2.29}$$

This information can be used to specify the intervals on which roots are located when the roots are computed numerically.

2.8 Interface Equation

The interface equation between the two phases is given by

$$\frac{\partial \theta_{liq}(\eta,\tau)}{\partial \eta}\Big|_{\eta=\zeta(\tau)} + \frac{d\zeta(\tau)}{d\tau} = \frac{\partial \theta_{sol}(\eta,\tau)}{\partial \eta}\Big|_{\eta=\zeta(\tau)}$$

We need to differentiate solutions for the temperature in both phases with respect to η and evaluate the derivatives at the interface $\eta = \zeta(\tau)$. Note that

$$\frac{d}{dz}J_0(z) = -J_1(z) \quad \text{and} \quad \frac{d}{dz}Y_0(z) = -Y_1(z)\tilde{\lambda}$$

Then

$$\frac{\partial \theta_{liq}(\eta,\tau)}{\partial \eta} = \sum_{n=1}^{\infty} A_n \, \mathrm{e}^{-\lambda_n^2 \tau}(-\lambda_n) J_1(\lambda_n \eta) - \frac{\dot{Q}}{2}\eta$$

$$\frac{\partial \theta_{sol}(\eta,\tau)}{\partial \eta} = \sum_{n=1}^{\infty} B_n \tilde{\lambda}_n \bar{f}_n(\tilde{\lambda}_n \eta) \, \mathrm{e}^{-\tilde{\lambda}_n^2 \tau} - \frac{\dot{Q}}{2}\eta + \left(\frac{\dot{Q}}{2} - Q''\right)\frac{1}{\eta}$$

where we introduce notation $\bar{f}_n$

$$\frac{d\tilde{f}_n(\tilde{\lambda}_n\eta)}{d\eta} = \tilde{\lambda}_n\bar{f}_n(\tilde{\lambda}_n\eta)$$

and

$$\bar{f}_n(\tilde{\lambda}_n\eta) = -J_1(\tilde{\lambda}_n\eta) + \frac{J_1(\tilde{\lambda}_n)}{Y_1(\tilde{\lambda}_n)}Y_1(\tilde{\lambda}_n\eta) \tag{2.30}$$

Then evaluating derivatives at the interface we get

$$\frac{d\zeta(\tau)}{d\tau} = \sum_{n=1}^{\infty} A_n\lambda_n J_1(\lambda_n\zeta)\,\mathrm{e}^{-\lambda_n^2\tau} + \sum_{n=1}^{\infty} B_n\tilde{\lambda}_n\bar{f}_n(\tilde{\lambda}_n\zeta)\,\mathrm{e}^{-\tilde{\lambda}_n^2\tau} + \left(\frac{\dot{Q}}{2} - Q''\right)\frac{1}{\zeta} \tag{2.31}$$

where

$$A_n = \frac{\int_0^{\zeta(\tau)}[\Phi_{liq}(\eta) - \theta_{liq,ss}(\eta)]J_0(\lambda_n\tau)\eta\,d\eta}{\int_0^{\zeta(\tau)} J_0^2(\lambda_n\eta)\eta\,d\eta}$$

$$B_n = \frac{\int_{\zeta(\tau)}^1(\Phi_{sol}(\eta) - \theta_{sol,ss}(\eta))\bar{f}_n(\tilde{\lambda}_n\eta)\eta\,d\eta}{\int_{\zeta(\tau)}^1[\tilde{f}_n(\tilde{\lambda}_n\eta)]^2\eta\,d\eta}$$

$$\lambda_n = \frac{z_{0n}}{\zeta(\tau)}, \quad \bar{f}_n(\tilde{\lambda}_n\eta) = -J_1(\tilde{\lambda}_n\eta) + \frac{J_1(\tilde{\lambda}_n)}{Y_1(\tilde{\lambda}_n)}Y_1(\tilde{\lambda}_n\eta)$$

$$\tilde{f}_n(\tilde{\lambda}_n\eta) = J_0(\tilde{\lambda}_n\eta) - \frac{J_1(\tilde{\lambda}_n)}{Y_1(\tilde{\lambda}_n)}Y_0(\tilde{\lambda}_n\eta), \quad n = 1, 2, \ldots$$

and $\tilde{\lambda}_n$ are the roots of

$$Y_1(\tilde{\lambda})J_0(\zeta\tilde{\lambda}) - Y_0(\zeta\tilde{\lambda})J_1(\tilde{\lambda}) = 0 \tag{2.32}$$

2.9 Quasi-Static Solutions

These are solutions that are time independent inside each phase. Dependence on time comes from the interface equation. Expressions for temperature in each phase can be obtained by letting $\tau \to \infty$ in (2.15) and (2.23). This eliminate infinite series terms and we obtain that

temperature coincides with steady state solutions we found earlier, namely,

$$\theta_{liq}(\eta) = \theta_{liq,ss}(\eta) = \frac{\dot{Q}}{4}(\zeta^2(\tau) - \eta^2)$$

$$\theta_{sol}(\eta) = \theta_{sol,ss}(\eta) = \frac{\dot{Q}}{4}\big(\zeta^2(\tau) - \eta^2\big) + \left(\frac{\dot{Q}}{2} - Q''\right)\ln\frac{\eta}{\zeta}$$

The quasi-static equivalent of the interface equation (2.31) is

$$\frac{d\zeta(\tau)}{d\tau} = \left(\frac{\dot{Q}}{2} - Q''\right)\frac{1}{\zeta} \tag{2.33}$$

We can see from equation (2.33) that $\frac{d\zeta(\tau)}{d\tau} > 0$ when $\frac{\dot{Q}}{2} > Q''$. In this case, ζ will increase with time and the interface will move to the right and we will have melting process. Similarly, when $\frac{\dot{Q}}{2} < Q''$, we have $\frac{d\zeta(\tau)}{d\tau} < 0$ and ζ will decrease resulting in front moving to the left. In this case, we would have solidification process.

Integrating equation (2.33) and using the initial condition $\zeta(0) = \zeta_0$, we find

$$\frac{d\zeta(\tau)}{d\tau} = \left(\frac{\dot{Q}}{2} - Q''\right)\frac{1}{\zeta}$$

$$\zeta d\zeta = \left(\frac{\dot{Q}}{2} - Q''\right)d\tau$$

$$\frac{\zeta^2}{2} = \left(\frac{\dot{Q}}{2} - Q''\right)\tau + \tilde{c}$$

$$\zeta^2 = (\dot{Q} - 2Q'')\tau + c$$

$$\zeta(\tau) = \zeta(0) \quad \Rightarrow c = \zeta_0^2$$

$$\zeta^2(\tau) = (\dot{Q} - 2Q'')\tau + \zeta_0^2$$

or

$$\zeta(\tau) = \sqrt{\left(\dot{Q} - 2Q''\right)\tau + \zeta_0^2} \tag{2.34}$$

This result shows that the interface in the quasi-static regime behaves like $\sqrt{\tau}$. It is also in agreement with results in [21] where quasi-static problem was studied by Crepeau and Siahpush.

CHAPTER 3

Numerical Solutions

In this chapter we solve the initial value problem for the interface equation (2.31) derived in the previous chapter. We consider two regimes: melting and solidification. To analyze them, we need initial conditions for both regimes. Let us suppose that the material is all in a single phase, solid or liquid, and the surfaces are at some constant temperature. Then, we turn on the internal heat generation and the temperature in the material begins to increase, until it just begins to melt. Under those conditions, the temperature profile within the material would be parabolic. Similar argument is used for the liquid phase. The internal heat generation causes a parabolic profile to occur within the material. As the material continues to heat up, it would begin to melt along the centerline, the location of the highest temperature. Therefore, we use the following initial conditions.

Initial conditions for melting are:

$$\text{at} \quad \tau = 0 \quad \zeta(\tau) = 0, \quad \Phi_{liq}(\eta) = 0, \quad \Phi_{sol}(\eta) = -\eta^2 \tag{3.1}$$

At $\tau = 0$ the whole system is fully solid – see Fig. 3.1. The dashed line $\Phi(\eta) = 0$ represents dimensionless melting temperature. As τ increases, the solid starts melting and the temperature increases and exceeds the melting threshold $\Phi(\eta) = 0$.

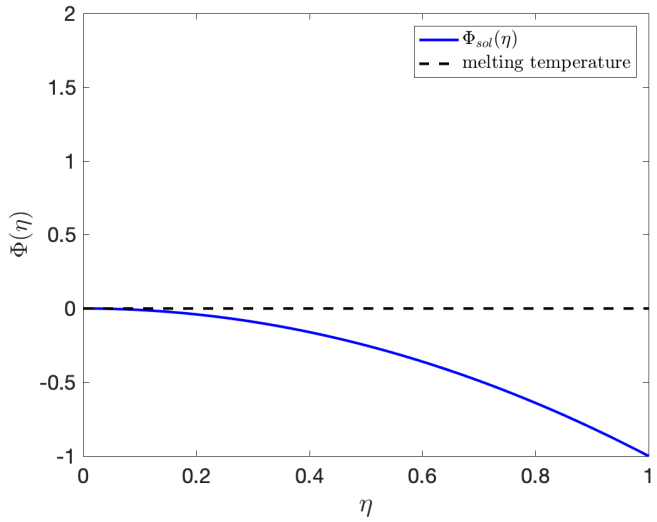

Figure 3.1: Initial condition for melting $\Phi_{sol}(\eta)$

Initial conditions for solidification:

$$\text{at} \quad \tau = 0 \quad \zeta(\tau) = 1, \quad \Phi_{liq}(\eta) = \frac{\dot{Q}}{4}(1-\eta^2), \quad \Phi_{sol}(\eta) = 0 \tag{3.2}$$

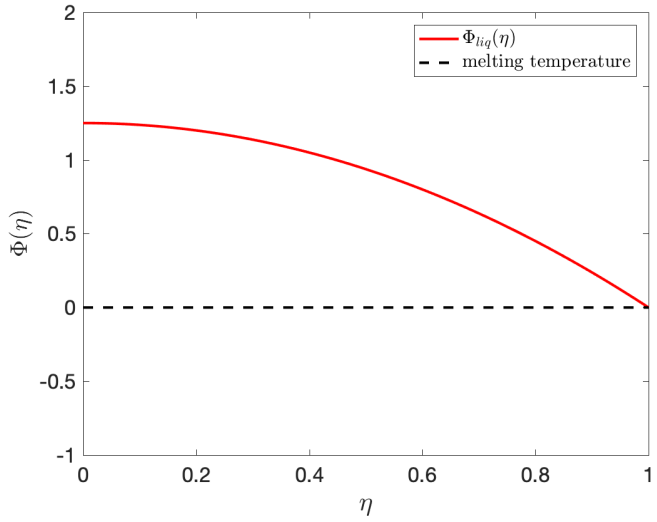

Figure 3.2: Initial condition for solidification $\Phi_{liq}(\eta)$

Here at $\tau = 0$ the whole system is fully liquid as shown in Fig. 3.2. As τ increases, the liquid starts solidifying and temperature moves below the melting threshold $\Phi(\eta) = 0$.

The initial value problem for the interface equation (2.31) subject to the initial conditions

(3.1) or (3.2) is solved with MATLAB software numerically using the solver ode23s. In order to evaluate the right hand side of equation (2.31) we need to compute first the eigenvalues in both liquid and solid phases. The eigenvalues λ_n in the liquid phase are related to the roots z_{0n} of the Bessel function $J_0(z)$ as was shown in the previous chapter. The roots z_{0n} are computed numerically. Eigenvalues $\tilde{\lambda}_n$ in the solid phase are found by solving equation (2.32) using a root finding method. In order to identify intervals where roots $\tilde{\lambda}_n$ are located, we use asymptotic roots (2.28) computed in the previous chapter. As was shown in (2.28) and (2.29), approximate roots and distance between them are

$$\tilde{\lambda}_n \approx \tilde{\lambda}_n^{as} = \frac{-\frac{\pi}{2} + \pi n}{1-\zeta}$$

and

$$\tilde{\lambda}_{n+1} - \tilde{\lambda}_n \approx \frac{\pi}{1-\zeta}$$

respectively. For each eigenvalue, its interval is taken to be

$$\left[\tilde{\lambda}_n^{as} - \frac{1}{4}\frac{\pi}{1-\zeta}, \tilde{\lambda}_n^{as} + \frac{1}{4}\frac{\pi}{1-\zeta}\right]$$

i.e. it is centered around the asymptotic value of the root and has 1/4 distance between roots to each side of the center. Then the Fourier-Bessel coefficients A_n and B_n, $n = 1, 2, \ldots$ are computed by numerical integration, the right hand side of the interface equation (2.31) is evaluated and used to advance the interface position $\zeta(\tau)$. Once eigenvalues λ_n and $\tilde{\lambda}_n$, the Fourier-Bessel coefficients A_n and B_n, interface position ζ are known, temperature profiles in both phases can be evaluated and analyzed. Since infinite series involve exponentially decaying τ terms and eigenvalues form increasing sequences, these series can be truncated, especially at later times and for higher indices n of eigenvalues. We typically use 10-20 terms in our simulations.

In Figs 3.3 and Fig. 3.4 we show plots of Bessel functions J_0, Y_0 and J_1, Y_1, respectively,

to demonstrate that they all oscillate, slowly decay and have infinitely many zeros.

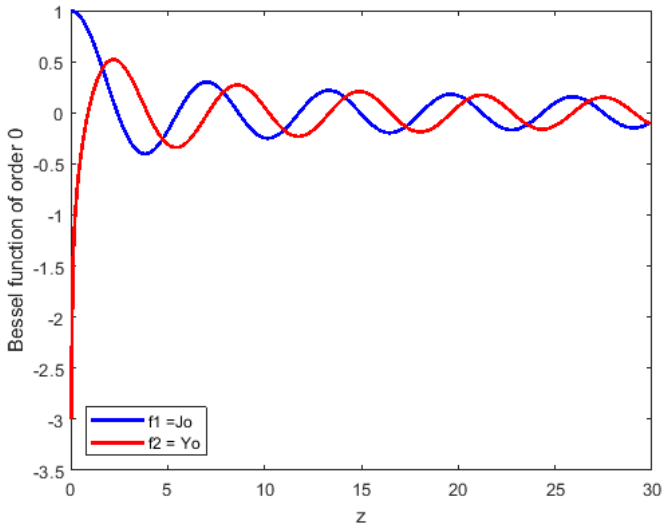

Figure 3.3: Graphs of Bessel functions $J_0(z)$ and $Y_0(z)$

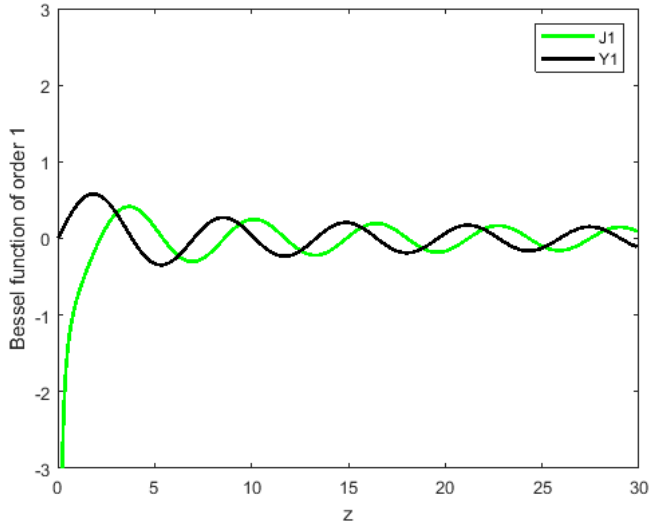

Figure 3.4: Graphs of Bessel functions $J_1(z)$ and $Y_1(z)$

In Fig. 3.5 we demonstrate our rootfinding approach by plotting the left hand side of equation (2.32), i.e. function $F(\lambda) = Y_1(\lambda)J_0(\zeta\lambda) - Y_0(\zeta\lambda)J_1(\lambda)$ as a function of λ for fixed $\zeta = 0.5$ together with asymptotic roots $\tilde{\lambda}_n^{as}$ (green circles) of this function and actual roots $\tilde{\lambda}_n$ (red stars). We can see that the asymptotic approximation of the eigenvalues $\tilde{\lambda}_n$ is very good even for low indices n. When the interface ζ is very close to the centerline, the difference between $\tilde{\lambda}_n^{as}$ and $\tilde{\lambda}_n$ should be taken care of more carefully. To compute the first root, the

location of the interval on which root is needs to be slightly adjusted to include the root and have the interval on the positive λ-axis completely.

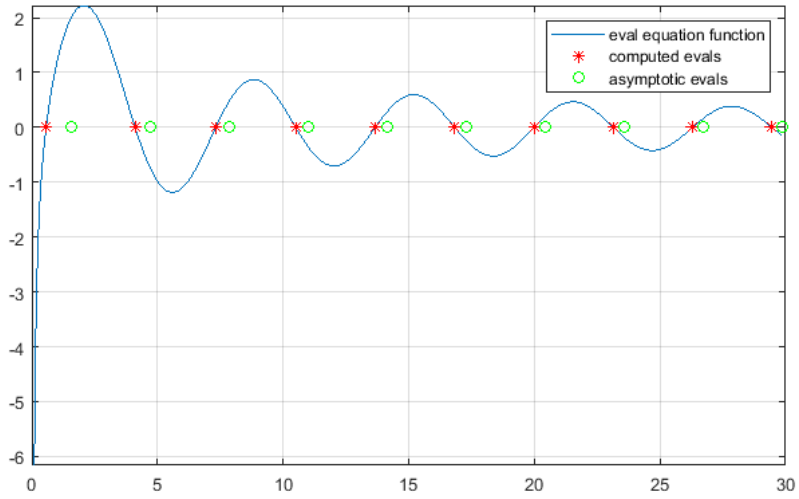

Figure 3.5: Graph of the left hand side $F(z)$ in (2.32) together with asymptotic approximations $\tilde{\lambda}_n^{as}$ of eigenvalues $\tilde{\lambda}_n$ and actual eigenvalues $\tilde{\lambda}_n$ with $\zeta = 0.5$

It follows from the expression of the slope (2.33) of the interface in the quasi-static case, i.e.

$$\frac{d\zeta(\tau)}{d\tau} = \left(\frac{\dot{Q}}{2} - Q''\right)\frac{1}{\zeta}$$

for melting to occur we would need

$$Q'' < \frac{\dot{Q}}{2}$$

so that the slope is positive and the interface would be moving to the right. Similarly, during the solidification we would require

$$Q'' > \frac{\dot{Q}}{2}$$

and the slope of the interface would be negative and the interface itself would be moving to the left.

In our simulations, we fix the internal heat generation at $\dot{Q} = 5$ and vary Q''. For each process, melting or solidification, we consider cases when Q'' and $\frac{\dot{Q}}{2}$ are close to each other or further apart. In the former case we expect that the interface would move slowly, whereas

in the latter case, the interface would reach either the outer boundary or the centerline relatively quickly.

3.1 Solidification

As the results for the quasi-static case suggest, in order to have solidification process, we need $Q'' > \frac{\dot{Q}}{2}$. This implies that the heat flux is strong enough to take heat generated internally out of the system at the boundary.

We consider solidification with $\dot{Q} = 5$ and $Q'' = 2.6$, 3 and 4. Fig. 3.6 shows the evolution of the interface (red curves) for these cases. For comparison, we plot the evolution of the interface in quasi-static case (black dashed curves). As expected from (2.34), the interface in the quasi-static case has a parabolic shape as a function of τ. As we can see, for early times the full and the quasi-static solutions follow the same shape and are very close to each other, since the heat flux Q'' is close to $\frac{\dot{Q}}{2}$. For $Q'' = 2.6$, the difference between full interface solution and quasi-static version is very small but as Q'' increases, the difference between them becomes evident as time τ increases. Fig. 3.7 considers bigger values of the heat flux: $Q'' = 4$ and 7.5. It is clear that full and quasi-static interfaces agree only for very early times and deviate quite a bit for later times. Further the value of Q'' from $\frac{\dot{Q}}{2}$ is, sooner curves start deviating from each other. We also see that the interface in the full problem moves a bit faster than the quasi-static equivalent, especially for higher values of Q''.

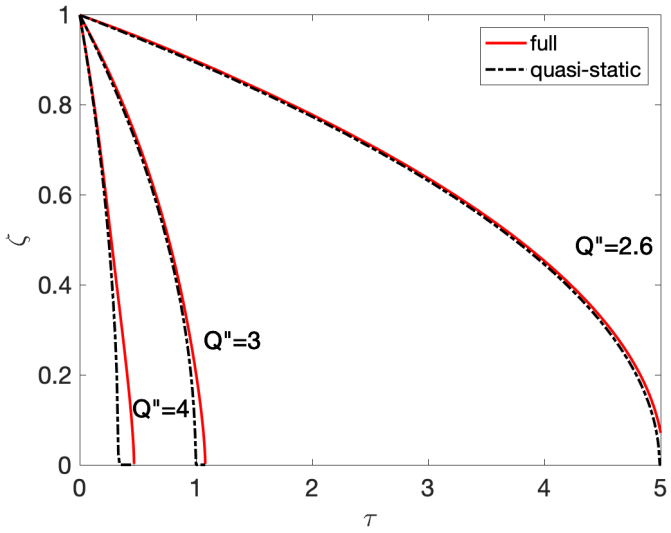

Figure 3.6: Evolution of the interface during solidification with $\dot{Q} = 5$ and $Q'' = 2.6, 3$ and 4

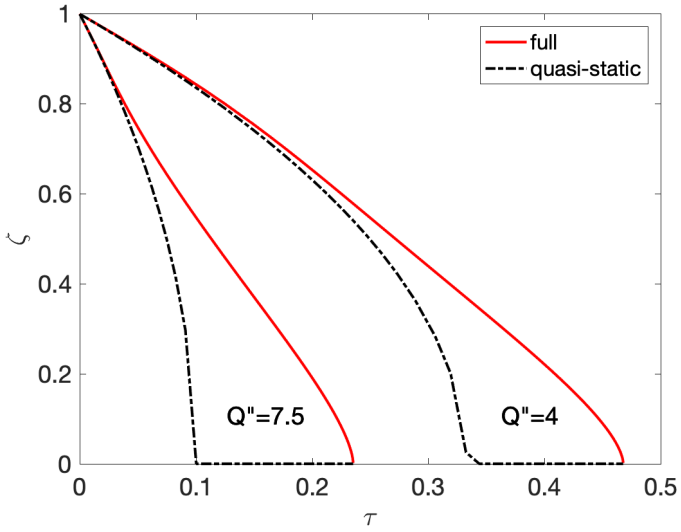

Figure 3.7: Evolution of the interface during solidification with $\dot{Q} = 5$ and $Q'' = 4$, and 7.5

In Fig. 3.8 we plot the evolution of the temperature during solidification with $Q'' = 2.6$. As we can see, the temperature profile in both phases remains concave down almost until the time the interface reaches the centerline. At later times, the temperature in the solid phase changes concavity and is concave up in the region adjacent to the interface. In Figs 3.9-3.11, the values of the heat flux are bigger: $Q'' = 3$, 4 and 7.5, respectively. As Q'' increases, concavity in the temperature in the solid phase changes at earlier times and when the interface is further from the centerline. The curvature in the concave up region also increases with Q''. Variation of

the temperature in the liquid phase does not depend on the value of the heat flux Q'' since we start our simulations from the same initial condition. At the same time, variation of the temperature in the solid region increases approximately by 3 times as Q'' increases from 2.6 to 7.5. Indeed, with $Q'' = 2.6$, temperature varies from 0 at $\tau = 0$ to -1.5 and with $Q'' = 7.5$ temperature goes down to about -4.2.

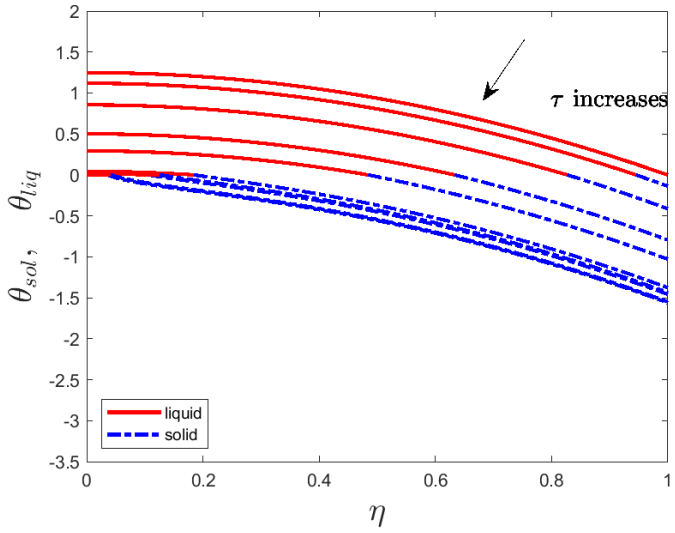

Figure 3.8: Evolution of temperature during solidification with Q''=2.6 and $\dot{Q} = 5$

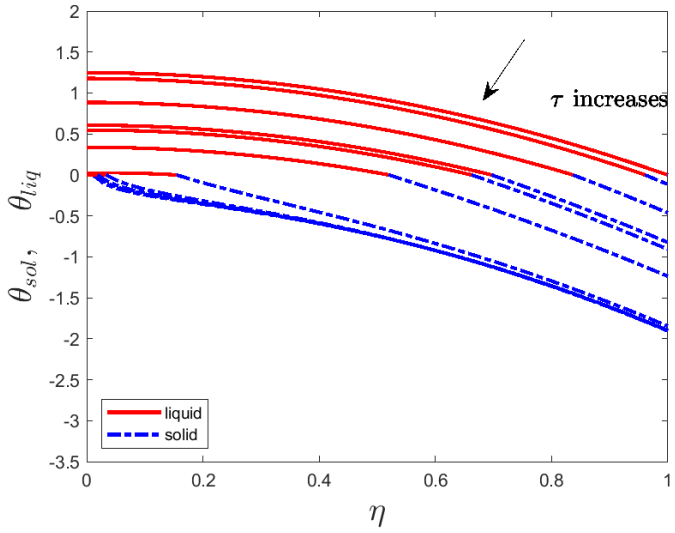

Figure 3.9: Evolution of temperature during solidification with Q''=3 and $\dot{Q} = 5$

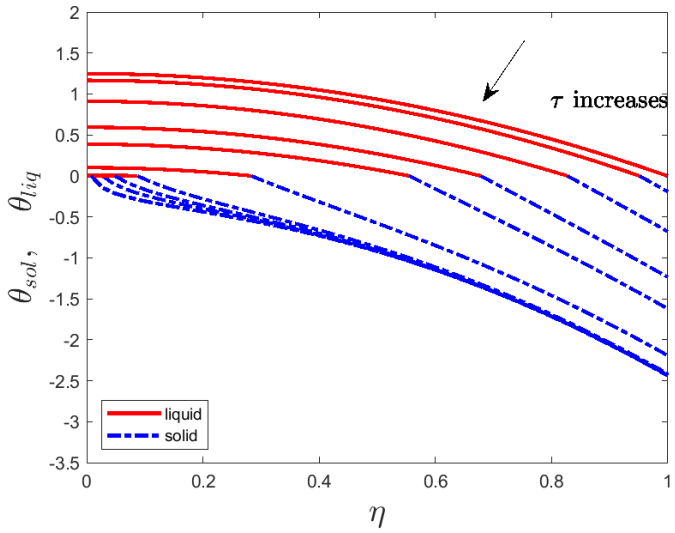

Figure 3.10: Evolution of temperature during solidification with Q''=4 and $\dot{Q} = 5$

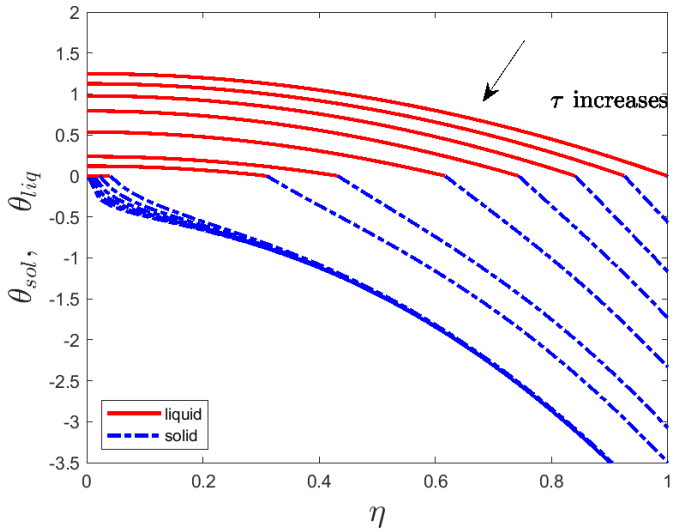

Figure 3.11: Evolution of temperature during solidification with Q''=7.5 and $\dot{Q} = 5$

3.2 Melting

For the melting process, we need $Q'' < \frac{\dot{Q}}{2}$. In this case, the heat flux at the outer boundary is not strong enough to compensate for the heat generated inside the cylinder, so the heat would continue to accumulate and enhance melting.

We set $\dot{Q} = 5$ as before and then study cases with the value of the heat flux Q'' close

to $\frac{\dot{Q}}{2}$ and then also farther away. The evolution of the interface ζ as a function of τ for cases when $Q'' = 1.5$, 2 and 2.4 is shown in Fig. 3.12. As can be seen from this figure, when Q'' is close to $\frac{\dot{Q}}{2}$, like in the case with $Q'' = 2.4$, the full and quasi-static solutions follow almost the same parabolic shape and are close to each other. As Q'' gets farther away from $\frac{\dot{Q}}{2}$ and decreases, the difference between the full and quasi-static curves increases but the overall shape remains about the same. Moreover, since in this case the heat flux at the boundary is weaker than the internal heat generation, the material's temperature increases quickly causing the melting to go faster. As a result, the interface between liquid and solid phases reaches the outer boundary of the cylinder quickly. Compared with $Q'' = 2.4$, when the interface is reached in about 5 times units, the same happens with $Q'' = 2.0$ or 1.5 in about one unit of time or about 5 times faster. In all three cases, the full melting process is a bit faster than the quasi-static one.

In Fig. 3.13, we show the evolution of the interface for $Q'' = 0.5$ and 1.5. These values are farther away from the equilibrium value $\frac{\dot{Q}}{2}$. The melting process is very fast and it takes about 0.4 and 0.7 units of time, respectively, to have the entire cylinder completely liquid. The full melting process is significantly faster than the quasi-static one. It is about twice faster for $Q'' = 0.5$.

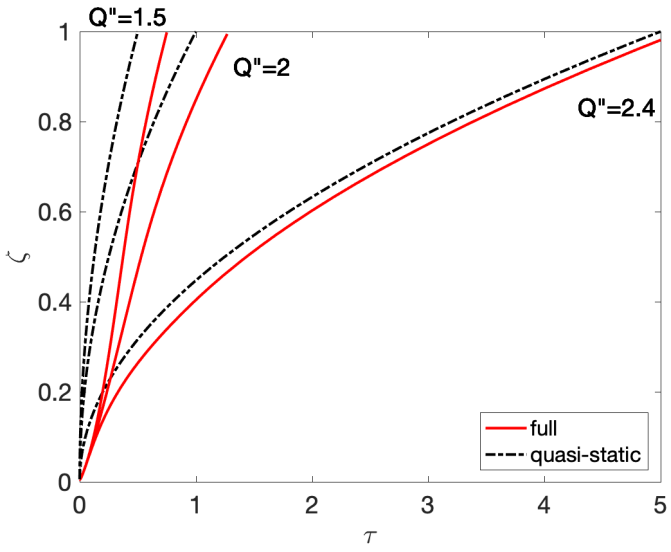

Figure 3.12: Evolution of the interface during melting with $\dot{Q} = 5$ and $Q'' = 1.5$, 2 and 2.4

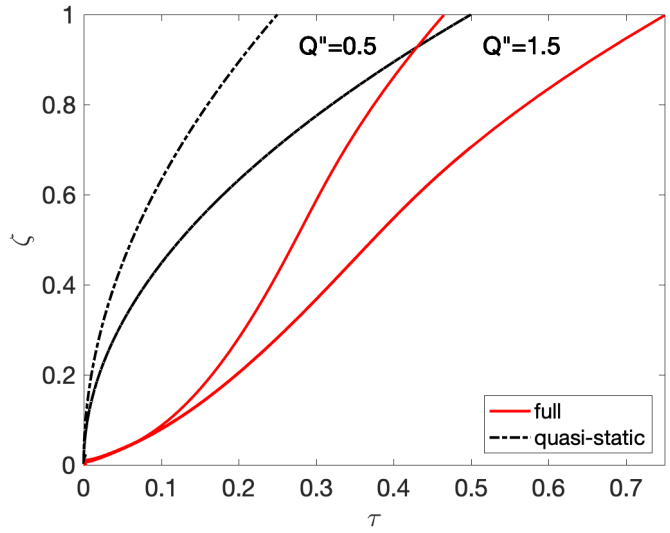

Figure 3.13: Evolution of the interface during melting with $\dot{Q} = 5$ and $Q'' = 0.5$ and 1.5

Next we show the evolution of temperature for the same values of the heat flux at the boundary. In Fig. 3.14, $Q'' = 2.4$ and it is close to $\frac{\dot{Q}}{2}$. We can see that as time τ increases, the overall temperature profile including both liquid and solid phases remains close to parabolic with a small change in the slope at the interface.

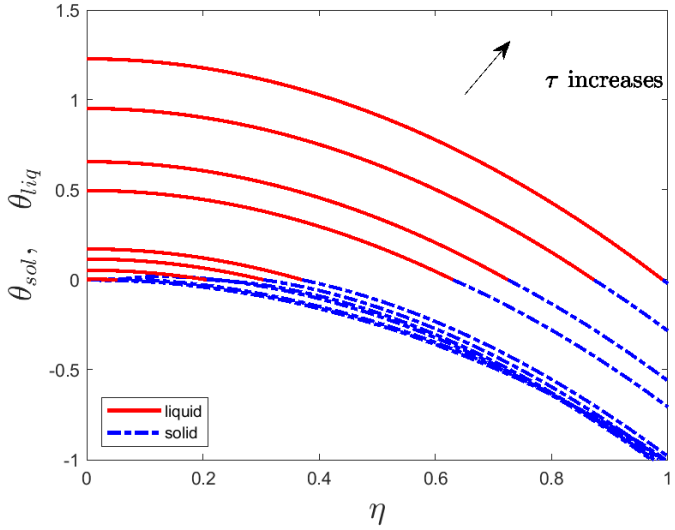

Figure 3.14: Evolution of temperature during melting with $Q'' = 2.4$ and $\dot{Q} = 5$

Next we decrease the heat flux to $Q'' = 2$. In this case, the internal heat generation allows melting to go faster. As we can see from Fig. 3.15, the temperature slopes at the interface

become more distinct. Moreover, we notice that the temperature in the solid phase at early times exceeds the melting threshold, which violates our modeling assumptions of having a phase change front at one point. This effect is called superheating in the solid phase. It was observed and studied in [35, 36]. This morphological change of the front suggests a formation of a "mushy" zone between phases and more general model should be employed. Welland [37] suggests using, for example, the phase field approach to capture the physics better. It should be noted that this unphysical superheating effect disappears at later times and the interface again exists only at one point later on. We can note that the superheated zone is relatively narrow and shrinks to a point by the time the interface reachers the middle of the path from the centerline to the outer boundary of the cylinder.

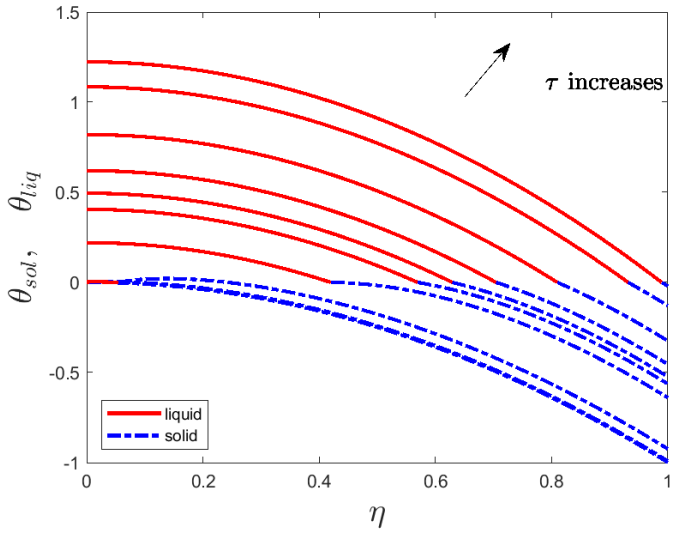

Figure 3.15: Evolution of temperature during melting with $Q'' = 2$ and $\dot{Q} = 5$

We decrease the heat flux further to $Q'' = 1.5$. As can be seen from Fig. 3.16, the "mushy" appears as well. It is wider in this case and shrinks to a point when the interface is further from the centerline than with $Q'' = 2$.

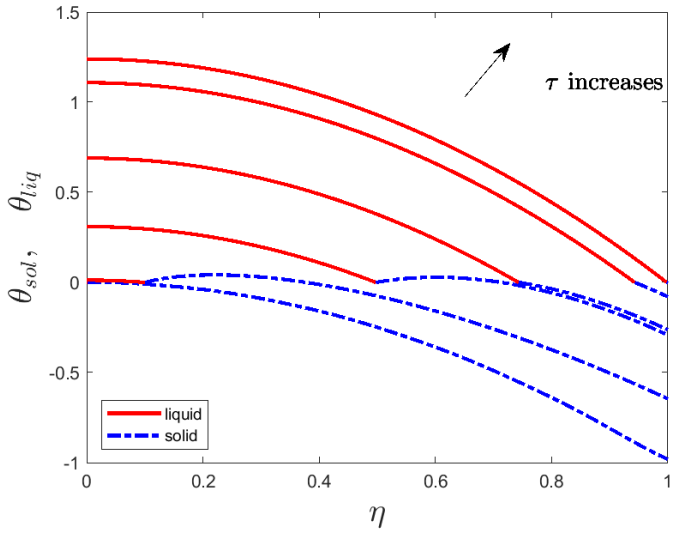

Figure 3.16: Evolution of temperature during melting with $Q'' = 1.5$ and $\dot{Q} = 5$

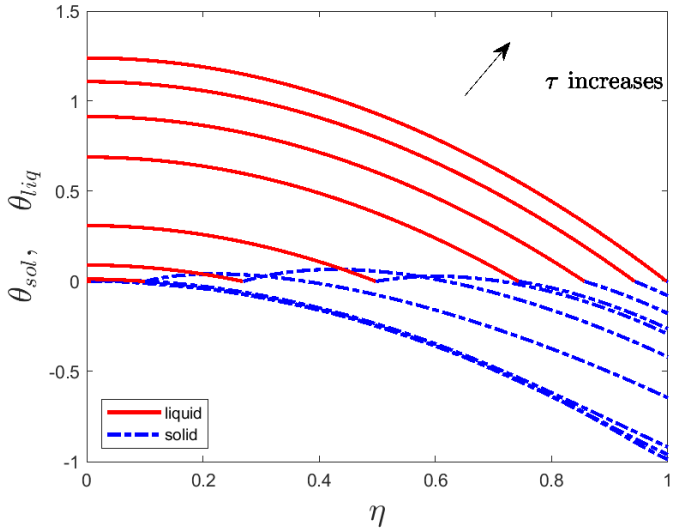

Figure 3.17: Evolution of temperature during melting with Q''=1.5 and $\dot{Q} = 5$

Finally we consider the case with $Q'' = 0.5$. As results in Fig. 3.18 suggest, the "mushy" is very wide here and converges to a point interface when the liquid phase front is very close to the outer boundary. This suggests that our model can be successfully used to predict the evolution of the interface and temperature during melting when the internal heat generation divided by 2 and the imposed heat flux on the boundary are not very far apart. For higher contrast between Q'' and $\frac{\dot{Q}}{2}$, more general models that include a possibility of a "mushy" zone should be employed.

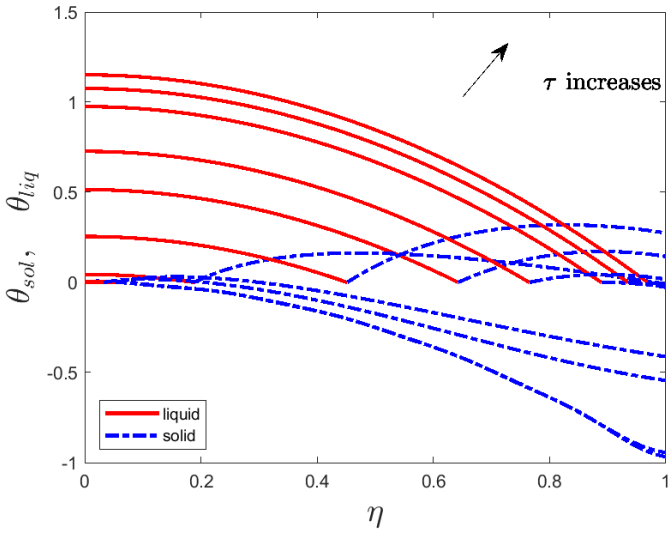

Figure 3.18: Evolution of temperature during melting with Q''=0.5 and $\dot{Q} = 5$

CHAPTER 4

Summary and Conclusions

In this thesis, the problem of solid liquid phase change in a cylinder with internal heat generation and prescribed heat flux at the outer boundary is solved analytically and numerically. Since we do not have a constant temperature at the outer boundary but prescribe the constant heat flux instead, the Stefan number is not introduced into the problem. Instead we introduce dimensionless heat flux coefficient at the boundary.

A first-order ordinary differential equation modeling the evolution of the interface between solid and liquid is derived. Because of the internal heat generation, the problem is nonhomogeneous and so the approach used involves the method of superposition to split the nonhomogenous problem into transient (homogenous) and steady-state (nonhomogenous). The transient problems in both phases are solved by the standard method of separation of variables and solving eigenvalue problems, while the steady state problems are solved by direct integration. The temperature in both phases is then found in terms of infinite series with Fourier-Bessel coefficients and exponentially decaying in time terms. The resulting initial value problem for the interface is solved numerically. Since the eigenvalues in both phases increases with index and temperature decay exponentially in time, just a few terms can be used to compute the solution. The obtained solutions are compared to quasi-static counterparts, which are steady-state solutions in each phase.

We consider two processes: solidification and melting. From the quasi-static case, we find that solidification or melting will occur if the heat flux at the boundary is less or greater than the half of the internal heat generation, respectively. This gives either strong enough heat flux at the boundary to overcome the internal heat generation and support solidification or weak heat flux to allow temperature inside the cylinder to increase due to the internal heat generation and promote melting.

We find that when the heat flux at the boundary is approximately the same as a half of the internal heat generation, we are close to the quasi-static regime and the interfaces for the full

and quasi-static problems are close to each other and both have parabolic shape. The overall temperature in both liquid and solid phases has almost the same slopes at the interface. As the difference between the heat flux and the half of the internal heat generation increases, the front between liquid and solid phases moves faster and the interface of the full problem significantly differ from the quasi-static counterpart. The interface of the full problem also moves faster than one of the quasi-static equivalent. Temperatures in liquid and solid phases have significantly different slopes at the interface. In case of melting with large difference between the heat flux and the half of the internal heat generation, the solutions for the temperature indicate a morphological change at the interface as it stops being at a single point. Instead we observe overheating in the solid phase with the temperature going above the melting point. This suggests formation of a "mushy" zone and perhaps more general model that takes into account a "mushy" zone should be employed.

Using these observations, we can conclude that given the internal generating heat, the heat flux at the boundary can be used to control the motion and speed of the interface between phases.

References

[1] G. Lamé, B. Clapeyron, Memoire sur la solidification par refroidissement d'un globe liquide, Annales Chimie Physique 47 (1831) 250–256.

[2] J. Stefan, Ueber die theorie der eisbildung, insbesondere ü ber die eisbildung im polarmeere, Sitzungsberichte deer k.k. Akademie der Wissenschaften in Wien, Mathematische-Naturwissenschaften, Abteilung II (1889) 965–983.

[3] V. Alexiades, A. D. Solomon, Mathematical Modeling of Melting and Freezing Processes, Hemisphere, 2008.

[4] L. Rubenstein, The Stefan Problem, AMS Pubs, Providence, 1971.

[5] L. C. Burmeister, Convective Heat Transfer, 2nd ed., Wiley, New York, 1993.

[6] R. M. Furzeland, A comparative study of numerical methods for moving boundary problems, IMA Journal of Applied Mathematics (Institute of Mathematics and Its Applications) 26 (4) (1980) 411–429.

[7] R. Viswanath, Y. Jaluria, Comparison of different solution methodologies for melting and solidification problems in enclosures, Numerical Heat Transfer, Part B: Fundamentals 24 (1) (1993) 77–105.

[8] N. N. Salva, D. A. Tarzia, Explicit solution for a Stefan problem with variable latent heat and constant heat flux boundary conditions, Journal of Mathematical Analysis and Applications.

[9] G. S. Lock, M. Ray, Latent Heat Transfer: An Introduction to Fundamentals, Developments in Chemical Engineering and Mineral Processing.

[10] S. C. Gupta, Chapter 1 - the Stefan problem and its classical formulation, in: The Classical Stefan Problem (2nd Edition), Vol. 45, Elsevier, 2018, pp. 1–35.

[11] S. C. Gupta, Chapter 10 - analysis of the classical solutions of Stefan problem, in: The Classical Stefan Problem (Second Edition), Vol. 45, Elsevier, 2018, pp. 251–295.

[12] R. Viskanta, Heat transfer during melting and solidification of metals, Journal of Heat Transfer 110 (4) (1988) 1205–1219.

[13] L. S. Yao, J. Prusa, Melting and Freezing, Advances in Heat Transfer (1989) 1–95.

[14] C. An, F. Moreira, J. Su, Thermal analysis of the melting process in a nuclear fuel rod, Applied Thermal Engineering 68 (2014) 133–143.

[15] Power reactor fuel, `http://www.nccp.ru/en/products/fuel_for_nuclear_power_plants/`, accessed: 2019-04-03.

[16] Y. Zhou, G. Shi, X.and Zhou, Exact solution for a two-phase stefan problem with power-type latent heat, Journal of Engineering Mathematics 110 (2018) 1–13.

[17] L. Tao, Exact solutions of some stefan problems with prescribed heat flux., Journal of Applied Mechanics, Transactions ASME 48 (4) (1981) 732–736.

[18] M. Z. Khalid, M. Zubair, M. Ali, An analytical method for the solution of two phase Stefan problem in cylindrical geometry, Applied Mathematics and Computation 342 (2019) 295–308.

[19] J. Prüss, J. Saal, G. Simonett, Existence of analytic solutions for the classical Stefan problem, Math. Ann. 338 (3) (2007) 703–755.

[20] F. Cheung, T. Chawla, D. Pedersen, The effects of heat generation and wall interaction on freezing and melting in a finite slab, International Journal of Heat and Mass Transfer 27 (1984) 29–37.

[21] J. Crepeau, A. Siahpush, Approximate solutions to the Stefan problem with internal heat generation, Heat and Mass Transfer / Waerme- und Stoffuebertragung 44 (7) (2008) 787–794.

[22] J. C. Crepeau, A. Siahpush, B. Spotten, On the stefan problem with volumetric energy generation, Heat and Mass Transfer/Waermeund Stoffuebertragung.

[23] A. Shrivastava, B. Williams, A. S. Siahpush, B. Savage, J. Crepeau, Numerical and experimental investigation of melting with internal heat generation within cylindrical enclosures, Applied Thermal Engineering 67 (1-2) (2014) 587–596.

[24] L. Barannyk, J. Crepeau, P. Paulus, A. Siahpush, Fourier-Bessel series model for the Stefan problem with internal heat generation in cylindrical coordinates, in: 26th International Conference on Nuclear Engineering ICONE26, July 22-26, London, England, 2018, pp. ICONE26–81009.

[25] L. Barannyk, S. Williams, O. Ogidan, J. Crepeau, A. Sakhnov, On the stefan problem with internal heat generation and prescribed heat flux conditions at the boundary, in: the ASME 2019 Summer Heat Transfer Conference, 2019, pp. HT2019–3703.

[26] R. Haberman, Applied Partial Differential Equations : With Fourier Series and Boundary Value Problems, Pearson, Boston, 2013.

[27] D. Poulikakos, Conduction Heat Transfer, Prentice-Hall, Englewood Cliffs, 1994.

[28] R. Haberman, Mathematical Models: Mechanical Vibrations, Population Dynamics, and Traffic Flow, Society for Industrial and Applied Mathematics, Philadelphia, 1998.

[29] E. Kreyszig, Advanced Engineering Mathemathics, 10th Ed., Hoboken, NJ : John Wiley, 2010.

[30] E. Kartashov, M. Krotov, Analytical solution of the single-phase Stefan problem, Mathematical Models and Computer Simulations 2 (1) (2009) 180–188.

[31] B. Lazhar, On the solutions of a Stefan problem with variable latent heat, Mathematical Problems in Engineering (2014) Art. ID 180764, 5.

[32] K. Ivaz, A. Beiranvand, Solving the Stefan problem with kinetics, Computational Methods for Differential Equations 2 (1) (2014) 37–49.

[33] G. Watson, A treatise on the theory of Bessel functions 2nd ed., The Macmillan Company : UP, Cambridge [England] New York, 1944.

[34] N. M. Temme, Special Functions: An Introduction to the Classical Functions of Mathematical Physics, John Wiley & Sons, Inc., Hoboken, NJ, USA:, 1996.

[35] A. Crowley, Numerical solution of Stefan problems, International Journal of Heat and Mass Transfer 21 (2) (1978) 215–219.

[36] D. R. Atthey, A finite difference scheme for melting problems, IMA Journal of Applied Mathematics 13 (1974) 353–366.

[37] M. J. Welland, Simulation of melting uranium dioxide nuclear fuel, PhD dissertation, Royal Military College of Canaday (2009).